



Cite this: *Chem. Soc. Rev.*, 2025, 54, 7913

Received 25th April 2025

DOI: 10.1039/d5cs00453e

[rsc.li/chem-soc-rev](http://rsc.li/chem-soc-rev)

## Combining biocatalytic and radical retrosynthesis for efficient chemoenzymatic synthesis of natural products

Hans Renata 

Retrosynthetic strategies are intimately tied to the tools and methods available at the time of their conception. Recent methodological advancements in both radical and biocatalytic reactions have created numerous possibilities for new and unconventional disconnections. Thus, it comes as no surprise that their applications in multi-step syntheses have allowed many complex molecules to be built in ingenious ways. This review summarizes recent case studies wherein radical-based and enzymatic transformations are combined strategically in multi-step sequences to achieve efficient total syntheses of complex natural products.

### 1. Introduction

The one-electron nature of radical reactions offers unique modes of reactivity for building complex molecules that are otherwise unavailable with two-electron processes. Spurred by the invention of new technologies in photoredox catalysis,<sup>1</sup> modern electrochemistry,<sup>2</sup> metal-catalyzed cross-coupling<sup>3</sup> and hydrogen atom transfer<sup>4</sup>—which offer milder reaction conditions and better functional group compatibility than

“classical” radical reactions—the field of radical chemistry has witnessed a major renaissance in recent years.<sup>5</sup> In addition to these advantages, modern radical chemistry also allows for the use of unconventional functional groups such as carboxylic acids<sup>6</sup> and alkenes<sup>4</sup> as viable radical precursors, opening the door for profoundly different bond disconnections during synthesis planning. In the same vein, biocatalytic retrosynthesis<sup>7</sup> has recently emerged as an enabling paradigm in chemical synthesis, owing to the unique selectivity profile of enzymatic reactions and the ever-increasing ability to modulate the activity and selectivity of enzymes with directed evolution and protein engineering. The transformative effects of this paradigm are manifest in the recent discoveries of new enzymes for site-selective oxidations,<sup>8</sup> the advent of new-to-nature biocatalytic reactions<sup>9</sup> and several high-profile reports<sup>10</sup> on the use of enzymatic cascades in the preparation of drug molecules and active pharmaceutical ingredients.

Recently, various research groups have managed to capitalize on the unique features of biocatalytic and radical retrosynthetic logic and strategically combine them to achieve efficient chemoenzymatic synthesis of complex natural products. Generally speaking, these cases can be divided into two categories: (1) using enzymatic cyclization to construct the core architecture of the target natural product, followed by radical-based chemical reactions to functionalize the core, or (2) using radical-based C–C bond formations to generate the core architecture of the target natural product, which is done in combination with enzymatic tailoring, usually oxidation, to install the requisite functional groups. Coincidentally, it should be noted there has been a heavy emphasis on applying these two chemoenzymatic approaches to terpenoid natural products. This review will be organized according to the two

Department of Chemistry, Rice University, BioScience Research Collaborative, Houston, TX, 77005, USA. E-mail: [hrenata@rice.edu](mailto:hrenata@rice.edu)



**Hans Renata**

*Hans Renata received his BA degree from Columbia University in 2008, conducting research with Professor Tristan Lambert. He earned his PhD from The Scripps Research Institute in 2013 under the guidance of Professor Phil Baran. After postdoctoral studies with Professor Frances Arnold at the California Institute of Technology, he started his independent career at The Scripps Research Institute in 2016. His research focuses on*

*the development of new biocatalytic methods and chemoenzymatic strategies to prepare complex, bioactive molecules. In July 2022, he took a position at Rice University as an Associate Professor and a CPRIT scholar.*



aforementioned categories. Additionally, we will present at the end several examples that involve non-terpenoid targets such as fatty acids and alkaloids.

## 2. Enzymatic cyclization followed by radical functionalization – introduction to terpene cyclases

Terpenoids are chemically and structurally diverse hydrocarbon-based natural products that arise from two 5-carbon precursors, isopentenyl diphosphate (IPP) and dimethylallyl diphosphate (DMAPP).<sup>11</sup> Initial head-to-tail coupling of IPP and DMAPP yields linear, achiral  $C_{5n}$  isoprenoid diphosphates ( $n = 1, 2, 3, \text{ etc.}$ ), which undergo various modes of cyclization by terpene cyclases to deliver products interesting three-dimensional architectures. Among the terpene cyclases,<sup>12</sup> class I terpenoid cyclases, such as bacterial pentalenene synthase, utilize a trinuclear metal cluster to activate pyrophosphorylated substrates, whereas class II terpenoid cyclases, such as SHCs, employ an active site side chain to protonate alkenes or epoxides for cyclization initiation.

Nature uses two pathways to generate the isoprenoid diphosphate precursors: the mevalonate (MVA) pathway<sup>13</sup> and (ii) the methylerythritol phosphate (MEP) pathway.<sup>14</sup> The mevalonate pathway begins with the conversion of acetyl CoA to acetoacetyl CoA, followed by an aldol coupling with another acetyl CoA molecule to generate (3S)-3-hydroxy-3-methylglutaryl CoA. Subsequent reduction affords (R)-mevalonate, which undergoes a series of reactions to provide isopentenyl diphosphate (IPP). The MEP pathway, sometimes referred to as the deoxyxylulose phosphate (DXP) pathway was only discovered in 1993, and is less well-studied relative to the MVA counterpart. The pathway starts with the union of pyruvate and D-glyceraldehyde-3-phosphate to produce DXP, which undergoes rearrangement in the presence of DXP reductase to provide 2C-methyl-D-erythritol-4-phosphate. Phosphorylation of this intermediate and reduction forms IPP. Finally, isomerization of IPP to DMAPP takes place in the presence of IPP isomerase, which becomes the starting point for further oligomerization to generate longer  $C_{5n}$  cyclization precursors, such as geranyl diphosphate (C10), farnesyl diphosphate (C15) and geranylgeranyl diphosphate (C20).

Several chemoenzymatic approaches to complex terpenoids featuring the use of terpene cyclases have recently been reported. The overall strategy is to employ a terpene cyclase for initial construction of the carbocyclic skeleton, followed by chemical tailoring to deliver the final terpenoid target(s). From a step economy perspective, the advantage here is obvious as the desired carbocyclic skeleton can be obtained in just one step. However, many of these enzymatic pathways, especially when carried out *in vivo*, are not efficient enough to generate sufficient materials to support a multi-step synthesis campaign. For this reason, it is often necessary to perform additional metabolic engineering on the bacterial and fungal host, typically to enhance precursor supply for the enzymatic cyclization. To date, engineering of the MVA pathway has been more widely

explored for this purpose than that of the MEP/DXP pathway. In recent years, several groups have taken advantage of the ability to readily access various terpene skeletons with terpene cyclases and used it in combination with modern radical reactions for efficient chemoenzymatic syntheses of complex terpenoids.

### 2.1. Chemoenzymatic synthesis of artemisinin

First isolated in 1972, the sesquiterpene artemisinin (**1**) is a widely-used small molecule for the treatment of malaria.<sup>15</sup> In fact, artemisinin-based combination therapies (ACTs) are now the standard treatment worldwide for malaria caused by *Plasmodium* species. The semi-synthetic artemisinin project was established in 2014 to improve the supply of artemisinin and lower its production cost through a two-stage approach involving microbial production of artemisinic acid (**2**), followed by its chemical conversion to artemisinin.<sup>16</sup> This project was highly successful and is often cited as an important milestone in metabolic engineering in the past two decades.

In 2006,<sup>17</sup> Keasling and coworkers engineered a *S. cerevisiae* strain that is equipped with an engineered MVA pathway, an amorphadiene synthase, and the P450 CYP71AV1 from *A. annua* to produce **2** with a titer of 100 mg L<sup>-1</sup> (Fig. 1). In this pathway, amorpha-4,11-diene (**3**) is produced by the synthase and gets converted by the P450 to **2**. Subsequent work by Paddon and coworkers<sup>18</sup> successfully doubled the titer production of **2** by overexpressing every enzyme in the MVA pathway up to ERG20 in an engineered *S. cerevisiae*. This achievement was complemented by optimization of the fermentation process to improve the titer further to >40 g L<sup>-1</sup>. In 2013,<sup>19</sup> Newman and coworkers reported that optimization of the oxidation of **3** to **2** could lead to a high-level production of **2** (25 g L<sup>-1</sup>) by yeast fermentation. Specifically, the researchers lowered the expression of *AaCPR*, which presumably affected the stoichiometry of CYP71AV1:*AaCPR* interaction, and introduced several auxiliary proteins such as cytochrome B5. Prior work in P450 biochemistry has suggested that the P450:CPR stoichiometry is important for optimal oxidation efficiency. Conversion of artemisinic acid to artemisinin has been widely studied and has even been conducted on process scale.<sup>20</sup> In the sequence, the *exo* methylene is first reduced, and the acid is converted to either the ester or the mixed anhydride (e.g., **5**), which was then subjected to a Schenck ene/rearrangement cascade with <sup>1</sup>O<sub>2</sub>—which has been proposed to proceed *via* radical mechanism—to furnish artemisinin. This last step has been studied extensively on process scale due to the need to develop special photochemical setups. For example, Sanofi has introduced a semibatch process with a recirculation loop while carefully choosing the reactor materials the identity of the photon source for optimal quantum photonic yield.

### 2.2. Chemoenzymatic synthesis of englerin A

Englerin A (**7**) is a plant sesquiterpenoid with potent nanomolar cytotoxicity against renal cancer cells,<sup>21</sup> which was later rationalized by its ability to activate the calcium channels TRPC4 and TRPC5.<sup>22</sup> In light of its potent bioactivity and unusual structure, more than 20 total and formal syntheses of **7** have been reported to date. In 2020, Liu, Christmann and coworkers<sup>23</sup> develop a



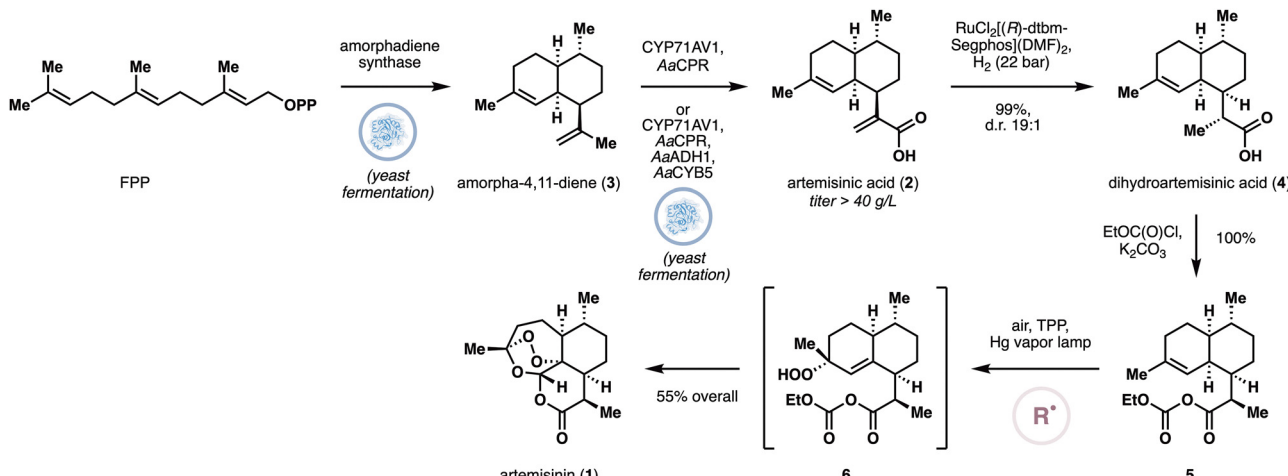


Fig. 1 Semisynthetic production of artemisinin through heterologous production of artemisinic acid and its chemical derivatization.

concise synthesis of 7 by relying on the heterologous production of guaia-6,10(14)-diene (8) in *S. cerevisiae*, followed by further chemical manipulations (Fig. 2A). Christmann, Dickschat and coworkers previously discovered STC5<sup>24</sup> as a class II sesquiterpene cyclase that converts FPP to 8. Due to the low isolation yields (4%) of the system, they tested additional sesquiterpene cyclases from filamentous fungi for guaia-6,10(14)-diene production in an *E. coli* strain that has been manipulated to overproduce FPP. The screening resulted in a slightly improved production of 8 at up to  $62.3 \text{ mg L}^{-1}$  with *E. coli* mutant G5, which contains the cyclase Fgj02895. Aiming at a more practical production, they further engineered the enzymes in the MVA pathway by CRISPR/Cas9 system in *S. cerevisiae*, and the titer of 8 was further increased to  $0.8 \text{ g L}^{-1}$  in 5 L fed-batch fermentation of *S. cerevisiae* YL06. Under Shenvi's conditions for hydrogen atom transfer-based olefin isomerization,<sup>25</sup> 8 was converted to diene 9, which was then subjected to a regio- and diastereoselective Sharpless dihydroxylation. The secondary alcohol was selectively acylated in the presence of acid chloride 11 and the remaining alkene was epoxidized with DMDO. *In situ* treatment of the epoxide with AcOH induced further cyclization to provide the core scaffold of englerin A. Introduction of the cinnamyl ester and removal of the TBDPS group completed the semisynthesis of 7.

### 2.3. Chemoenzymatic synthesis of schisanwilsonene A

The Xiang group has also developed an alternative approach (Fig. 2B) to heterologously produce guaia-6,10(14)-diene (8),<sup>26</sup> which used *E. coli* as the heterologous host. Specifically, the researchers employed a two-plasmid system wherein the MVA pathway was incorporated in the vector pACYCDuet-T1-B1 while the FPP synthase (FPPS) ERG20 and the sesquiterpene synthase STC5 were encoded in the vector pETDuet-ERG20-STC5. This system delivered 8 with a titer of  $119.4 \text{ mg L}^{-1}$ . While the terpene starting point is identical to that of Liu *et al.*, the Xiang group developed an alternative sequence to convert it to 7. Firstly, *m*CPBA was used to selectively epoxidize the trisubstituted olefin. *Exo*-to-*endo* isomerization of the remaining alkene was achieved under MHAT-based conditions, which was

followed by dihydroxylation and transannular cyclization in the presence of HCl to afford 17. Two sequential esterifications and deprotection of the PMB protecting group completed their synthesis of englerin A.

Using a similar heterologous expression system, the Xiang group has also reported a two-stage synthesis of (+)-schisanwilsonene A (20, Fig. 2C).<sup>27</sup> Firstly, introduction of the terpene cyclase IDS<sup>28</sup> in place of STC5 led to the accumulation of (+)-isodauc-8-en-11-ol (21) with a titer of  $1.16 \text{ g L}^{-1}$ . Under MHAT conditions for alkene isomerization, 21 was converted to 22 in 23% yield. Allylic oxidation of 22 with  $\text{SeO}_2$  and *t*BuOOH completed the synthesis of 20.

### 2.4. Chemoenzymatic synthesis of eunicellane and germiane diterpenoids

Eleutherobin (23) is a coral diterpene that possesses the ability to interfere with tubulin polymerization dynamics.<sup>29</sup> In light of its cytotoxicity, a number of synthetic studies have been performed to prepare eleutherobin and its unnatural derivatives. While these studies have generated valuable structure–activity relationship insights,<sup>30</sup> they generally employed lengthy sequences with low synthetic efficiency and overall yield. In 2022,<sup>31</sup> Schmidt and co-workers discovered coral terpene cyclases that produce the general eunicellane skeleton of eleutherobin and cembrene, providing an initial foothold for future synthetic biology approach to produce these diterpenoids. Their effort began with the sequencing and analysis of the metatranscriptome of *E. caribaeorum*, the soft coral producer of eleutherobin. While BLAST analysis did not identify any putative terpene cyclase, the use of hidden Markov model search recognized eight putative terpene cyclases. The authors further observed the colocalization of a terpene cyclase gene (called EcTPS1) with a P450-encoding gene and an acyltransferase-encoding gene in a biosynthetic gene cluster, which is consistent with the likely steps in eleutherobin biosynthesis. To lend support to this hypothesis, EcTPS1 was heterologously expressed in *E. coli* and was found to produce convert GGPP to the known eunicellane<sup>32</sup> klysplexin R (24).

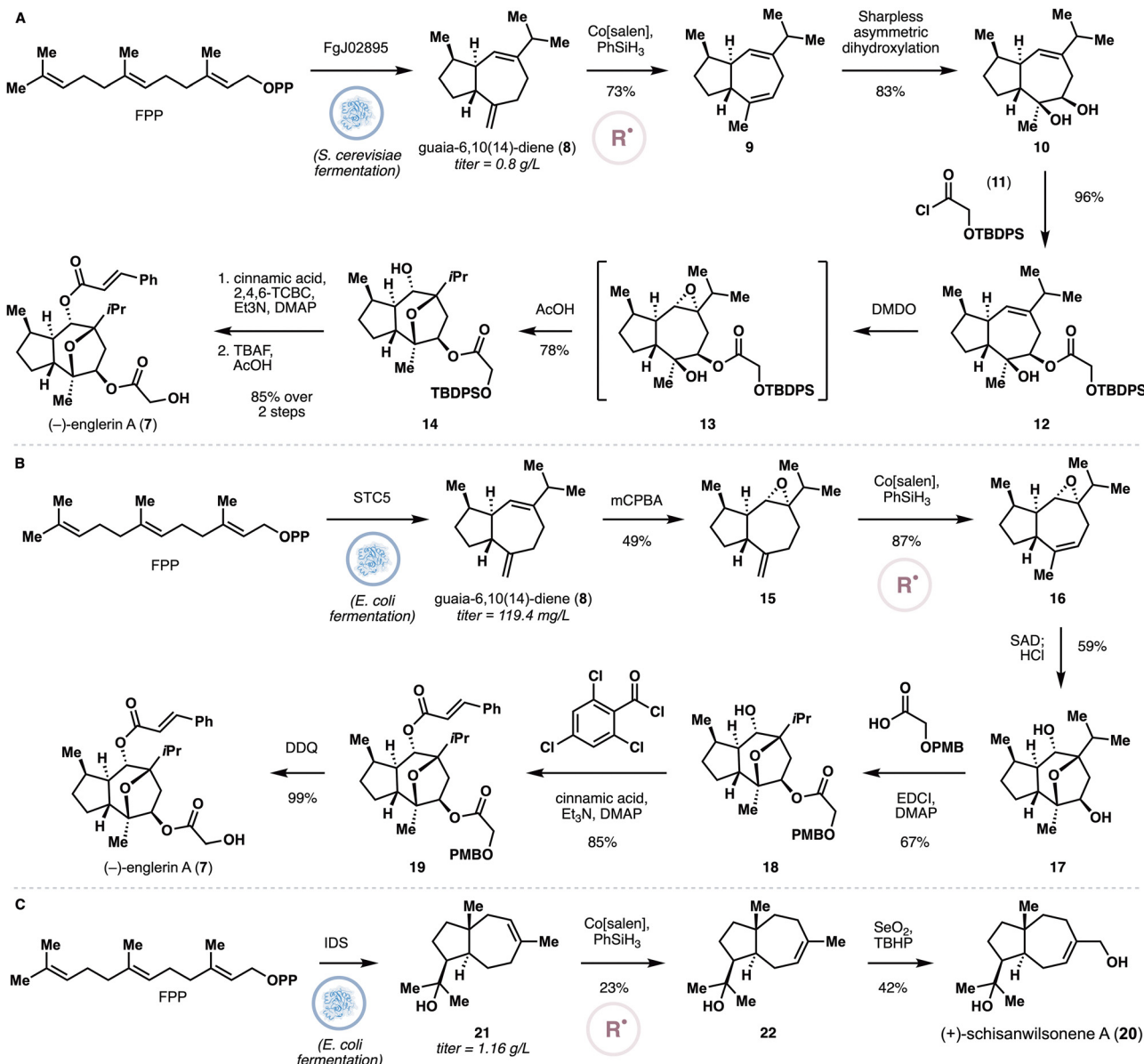


Fig. 2 (A) Chemoenzymatic synthesis of englerin A by Liu, Christmann and coworkers. (B) Chemoenzymatic synthesis of englerin A by Xiang and coworkers. (C) Xiang's chemoenzymatic synthesis of schisanwilsonene A.

Scaled-up fermentation of EcTPS1 reaction afforded klysimplexin R (24) with an average titer of  $77 \text{ mg L}^{-1}$ , which was used as a starting point for the divergent synthesis of additional coral diterpenoids (Fig. 3).<sup>33</sup> The C6–C7 alkene was selectively epoxidized with DMDO to produce a single diastereomer (25), which was found to have identical spectral data but opposite stereoconfiguration to solenopodin C. The same reaction converted 26 to a product (27) that displayed identical spectral data but opposite stereoconfiguration to klysimplexin Q. Under acidic conditions, 25 underwent transannular cyclization to provide two products with the gersemiane skeleton (28 and 29). Alternatively, sequential dihydroxylation of the C6–C7 alkene and TFDO-mediated epoxidation of the C2–C3 alkene afforded epoxide 31, which was treated with PTSA to induce

transannular etherification to form 32. Under MHAT conditions,<sup>25</sup> klysimplexin R could also be transformed to three products. Two of these products have the germiane skeleton, and the last one (33) is a regioisomer of eunicellol A. Finally, 24 was found to undergo  $^1\text{O}_2$  ene reaction at the C6–C7 alkene to form two alcohol diastereomers, 34 and 35, after reduction with  $\text{PPh}_3$ .

## 2.5. Chemoenzymatic synthesis of (+)-isoagatholactone, (+)-spongian-16-one and 3-deoxychevalone A

In contrast to class I terpene cyclases, class II terpene cyclases, use an aspartic acid side chain as a Brønsted acid to protonate alkenes or epoxides to initiate cyclization. Responsible for the conversion of squalene to hopene and hopanol, squalene



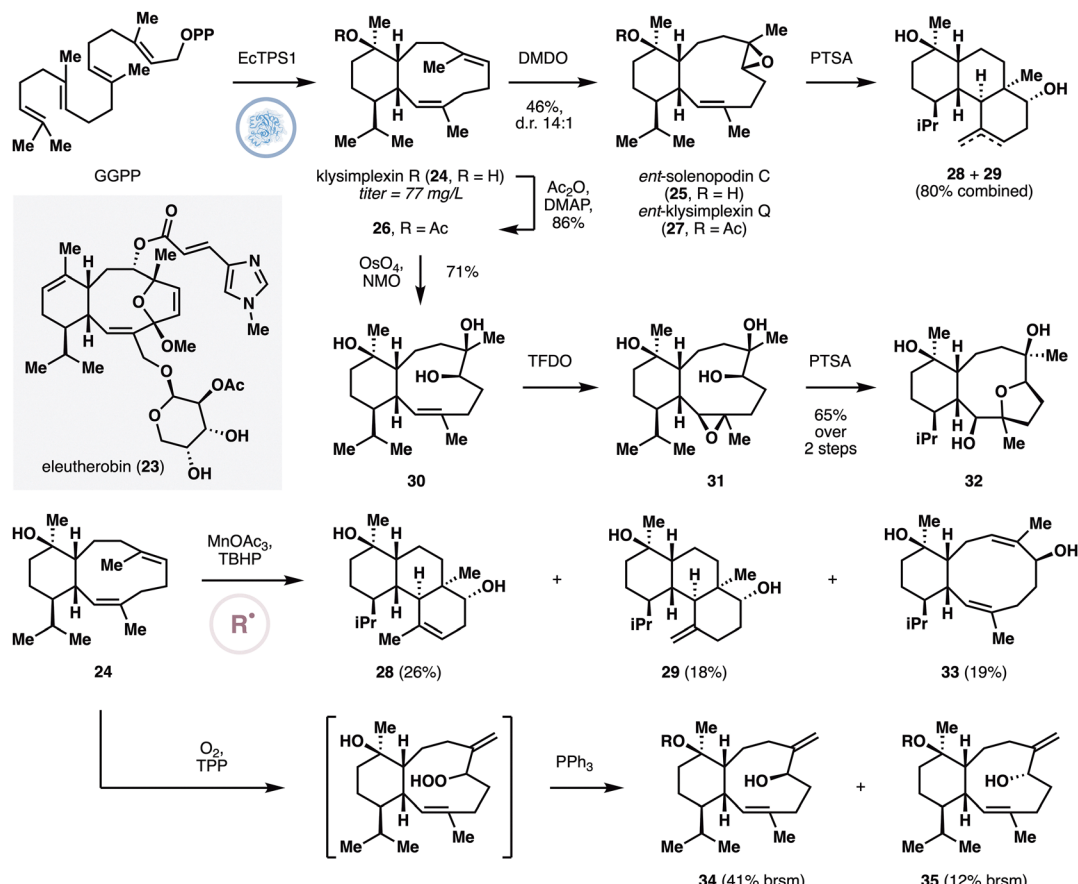


Fig. 3 Enzymatic cyclization of GGPP to klysimplexin R and its conversion to oxidized eunicellanes and the germiane skeleton by Scesa and Schmidt.

hopene cyclases (SHC) are among the most-studied class II cyclases.<sup>34</sup> Over the years, the Hauer group were able to harness this cyclization mode for non-native polyene cyclization through enzymatic Brønsted acid catalysis.<sup>35</sup> Several engineered variants of an SHC from *Alicyclobacillus acidocaldarius* (*AacSHC*) are able to accept alkenes, epoxides and carbonyls to form a diverse range of polycyclic ring systems.<sup>36</sup> More recently, Xiang and co-workers were able to capitalize on the promiscuity of *AacSHC* in the chemoenzymatic synthesis of (+)-isoagatholactone (36), (+)-spongian-16-one (37) and 3-deoxychevalone A (38, Fig. 4).<sup>37</sup> The synthesis began with enzymatic polyene cyclization of geranylgeraniol (39) with wild-type *AacSHC*, which was previously reported to proceed in 12% yield. In the authors' hands, the desired compound 40 was indeed obtained, but several side products were also detected, namely hydrated products 41 and 42, and the alkene isomer 43. At this stage, the authors performed *in silico* docking to identify several active site residues as candidates for directed evolution, which eventually led to variant 215G2. Containing mutations M132R, A224V and I432T, 215G2 catalyzed the formation of 40 with 34% isolated yield at 0.01 mol% enzyme loading. Allylic oxidation on 40, followed by treatment with Fetizon's reagent produced (+)-isoagatholactone (36), which was converted to (+)-spongian-16-one (37) *via* hydrogenation of 36 in the presence of RANEY® nickel. Finally, 42 was oxidized to the corresponding aldehyde (45), which was coupled

with 46 in a formal [3+3] reaction to deliver pyrone 48. Hydrogenation of 48 with Shenvi's conditions<sup>38</sup> proceeded with excellent chemo- and diastereoselectivity to complete the synthesis of 3-deoxychevalone A (38).

## 2.6. Divergent cross-coupling of albicanol to *ent*-chromozonarol, mycoleptodiscin A and pelorol

Earlier this year (2025), the Li and Dong groups reported a collaborative effort to synthesize several meroterpenoids through divergent cross-coupling from simple drimane precursors (Fig. 5), such as drimenol (49) or albicanol (50).<sup>39</sup> The premise of the approach is to enlist the use of terpene synthases to generate the drimane precursors, which would contain suitable chemical handles for subsequent cross-couplings. Similar to some of the previous case studies, the authors needed to come up with an approach to optimize the titer yield for the drimane precursors. Having previously developed a PhoN-IPK system<sup>40</sup> to boost the 5-carbon precursor supply for terpene synthases, the authors applied this system in combination with the drimenol synthase SsDMS. Unfortunately, this approach only resulted in a titer yield of 15 mg L<sup>-1</sup>. To address this issue, the authors employed a two-pronged optimization strategy. Firstly, SsDMS was artificially fused with a nudix hydrolase to enhance the hydrolysis of the diphosphate group from the initial terpene cyclization intermediate. This fusion strategy was found to



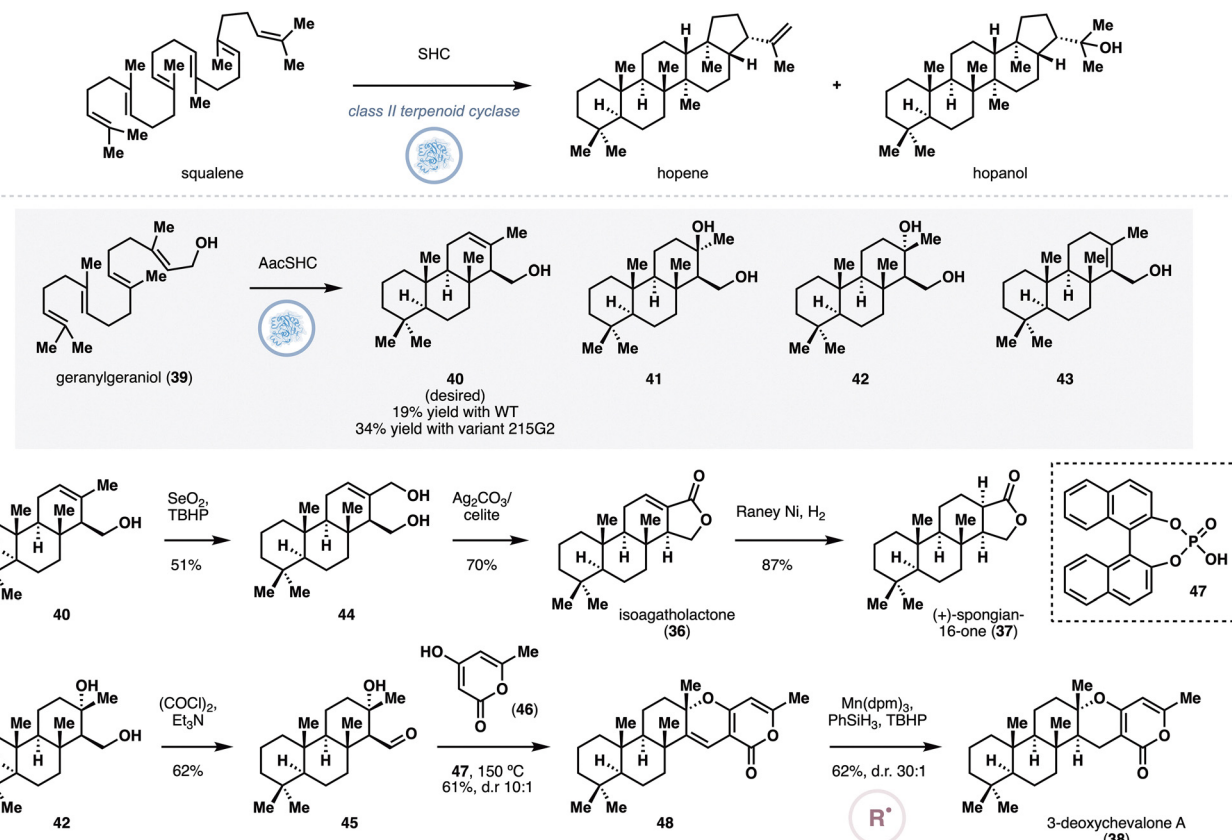
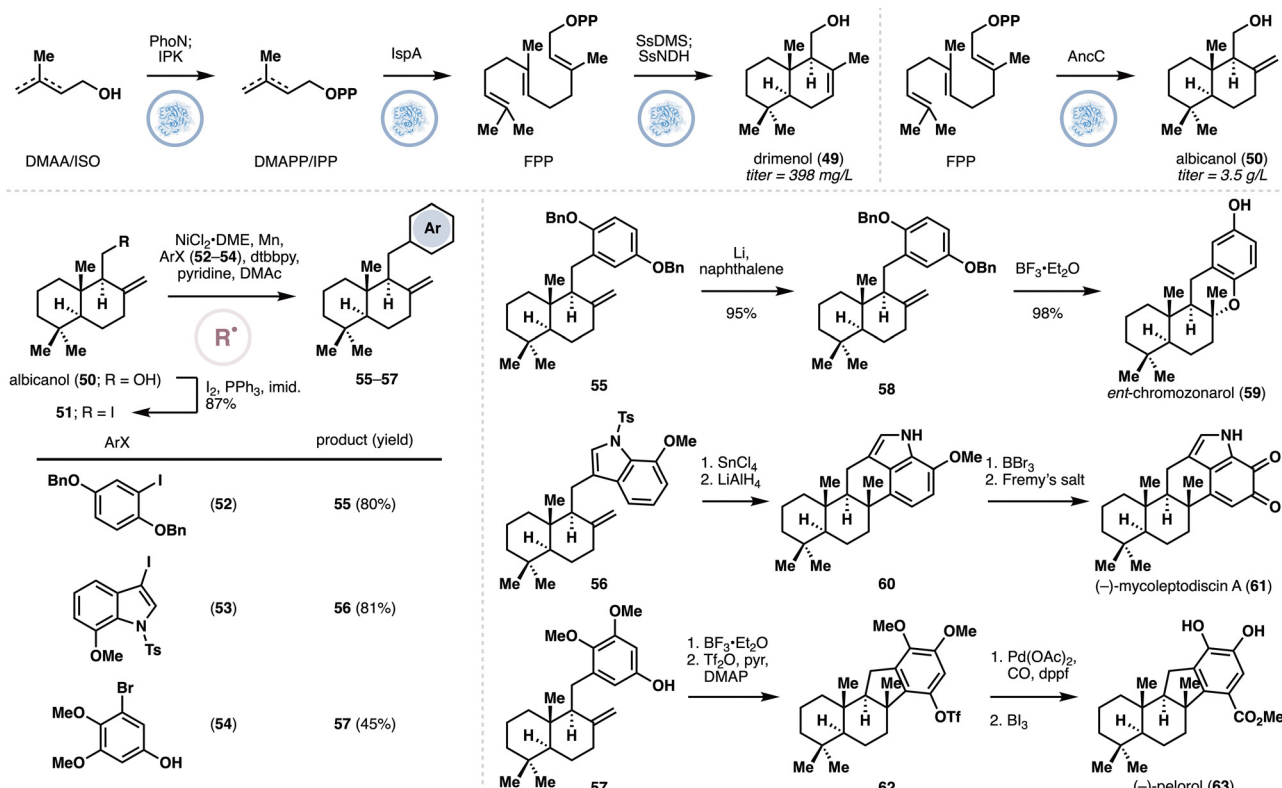


Fig. 4 Enzymatic cyclization of geranylgeraniol with engineered AacSHC and conversion of the cyclization products to isoagatholactone, spongian-16-one and 3-deoxychevalone A by Xiang and co-workers.

improve the product titer to 68–111 mg L<sup>−1</sup>, depending on the identity of the linker used.<sup>41</sup> As PhoN catalyzes reversible phosphorylation and hydrolysis reactions on dimethylallylalcohol/isopentenol, a rational engineering approach was pursued to boost the forward phosphorylation reaction under the hypothesis that introducing positive charges in the active site vicinity will improve interactions with the phosphate group. This approach was complemented with an alignment-based mutagenesis and the combined efforts identified three mutations, E122R, T157K and R160K, which led to a titer yield of 398 mg L<sup>−1</sup>. Replacement of SsDMS with the albicanol synthase AncC<sup>42</sup> allowed for an efficient production of albicanol (50) at a comparable titer. Most notably, a maximum titer of 3.5 g L<sup>−1</sup> of albicanol could be achieved by conducting the biotransformation in a bioreactor with exogenous feeding of isopentenol. The albicanol so produced was used as a starting point for divergent cross-couplings, specifically with nickel catalysis under Weix's conditions,<sup>43</sup> which are known to proceed through single electron pathways. Thus, conversion of 50 to the corresponding iodide (51) under Appel conditions, was followed by cross-couplings with the appropriate aryl iodide partners (52–54). Straightforward functional group manipulations completed the chemoenzymatic syntheses of *ent*-chromazonarol (59), mycoleptodiscin A (61) and pelorol (63).

### 3. The use of oxygenases for skeletal functionalization

One of the hallmarks of natural product biosynthesis is the involvement of various oxygenases in scaffold tailoring. While the resulting hydroxylation patterns may hold the key for potent biological activities, they also present additional structural complexity and potential chemoselectivity problems for chemical synthesis. Given the wealth of natural oxygenases, a number of research groups have begun to look for enzymatic solutions to address this challenge. While Nature has evolved a wide range of enzyme (super)families for oxidative chemistry, the two major superfamilies that have seen widespread use in organic synthesis are the P450s<sup>44</sup> and the non-heme iron dioxygenases (NHDs).<sup>45</sup> Though the two superfamilies use entirely different cofactors and rely on disparate mechanisms for dioxygen activation (Fig. 6), they share one common feature, that is the generation of a highly reactive Fe(IV)–oxo species for oxidative chemistry. This species is capable of performing a wide range of transformations, including C–H hydroxylation, desaturation, biaryl coupling and epoxidation, usually with high levels of site-, stereo- and chemoselectivity, which present a strategic advance in the context of complex molecule synthesis. To date, several strategies have been developed to realize the intended enzymatic oxidations, including transcriptomic



**Fig. 5** Enzymatic production of drimenol and albicanol and diversification of albicanol to ent-chromozonanol, mycoleptodiscin A and pelorol via radical cross-couplings by Li, Dong and co-workers.

analyses to discover new oxygenases, repurposing and engineering of known oxygenases from the native biosynthetic pathways, or screening of known promiscuous oxygenases such as P450BM3 variants.<sup>46</sup> In turn, the oxidation precursors could

be obtained either commercially or through chemical or biological synthesis (*i.e.* heterologous expression). Several research groups have recently taken advantage of the unique features of enzymatic oxidations and use them in combination with

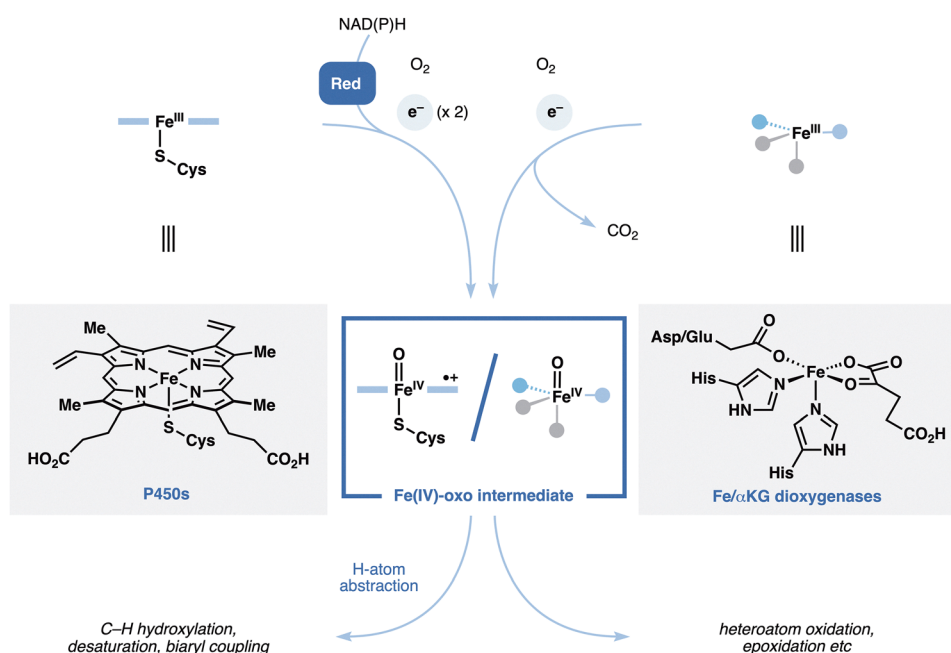


Fig. 6 Overview of reaction mechanisms for the P450s and Fe/αKG dioxygenases

modern radical reactions for skeletal construction or modification to achieve efficient chemoenzymatic synthesis of complex natural products.

### 3.1. Chemoenzymatic synthesis of meroterpenoids by combining biocatalytic oxidation and modern radical transformations

Commonly used as fragrance components, sclareolide and sclareol have also been widely used as starting materials in chiral pool synthesis,<sup>47</sup> particularly towards terpenoid targets that contain a labdane substructure. For example, the Baran group has reported the conversion of sclareolide to 'boronosclareolide', which was used as a divergence point to prepare several phenol-containing meroterpenoids.<sup>48</sup> Nevertheless, many labdane-containing targets with additional hydroxylation at C3 remain inaccessible with this semisynthetic approach, as chemical methods for direct C–H oxidation would proceed at the undesired C2 position due to stereoelectronic effects.<sup>49</sup>

An engineered P450BM3 variant, II-H8, was reported by Fasan and co-workers to catalyze a regio- and stereoselective C3 hydroxylation of sclareolide (**64**) in 83% yield, though the reaction was performed under dilute conditions (50 mg scale *in vitro* reaction with 1 mM substrate concentration).<sup>50</sup> Using this report as a starting point, the Renata group examined other P450BM3-based catalysts for the same reaction on sclareolide, but ran their screen on a larger scale at higher substrate concentration (5 mM).<sup>51</sup> A small alanine-scanning library was generated from a P450BM3 variant called 1857, which led to the discovery of a key mutation V328A for improved C3 hydroxylation activity. On gram scale reaction, oxidation of **64** with lysates of *E. coli* expressing 1857 V328A (also called "BM3 MERO1") provided 60–70% isolated yield of the desired product (**65**, Fig. 7A). Several routine steps converted **65** to aldehyde **66** or **67**, which was coupled with various aromatic fragments in a formal [3+3] annulation (Fig. 5B). Under Shen-  
vi's MHAT conditions,<sup>38</sup> hydrogenation of the [3+3] adducts

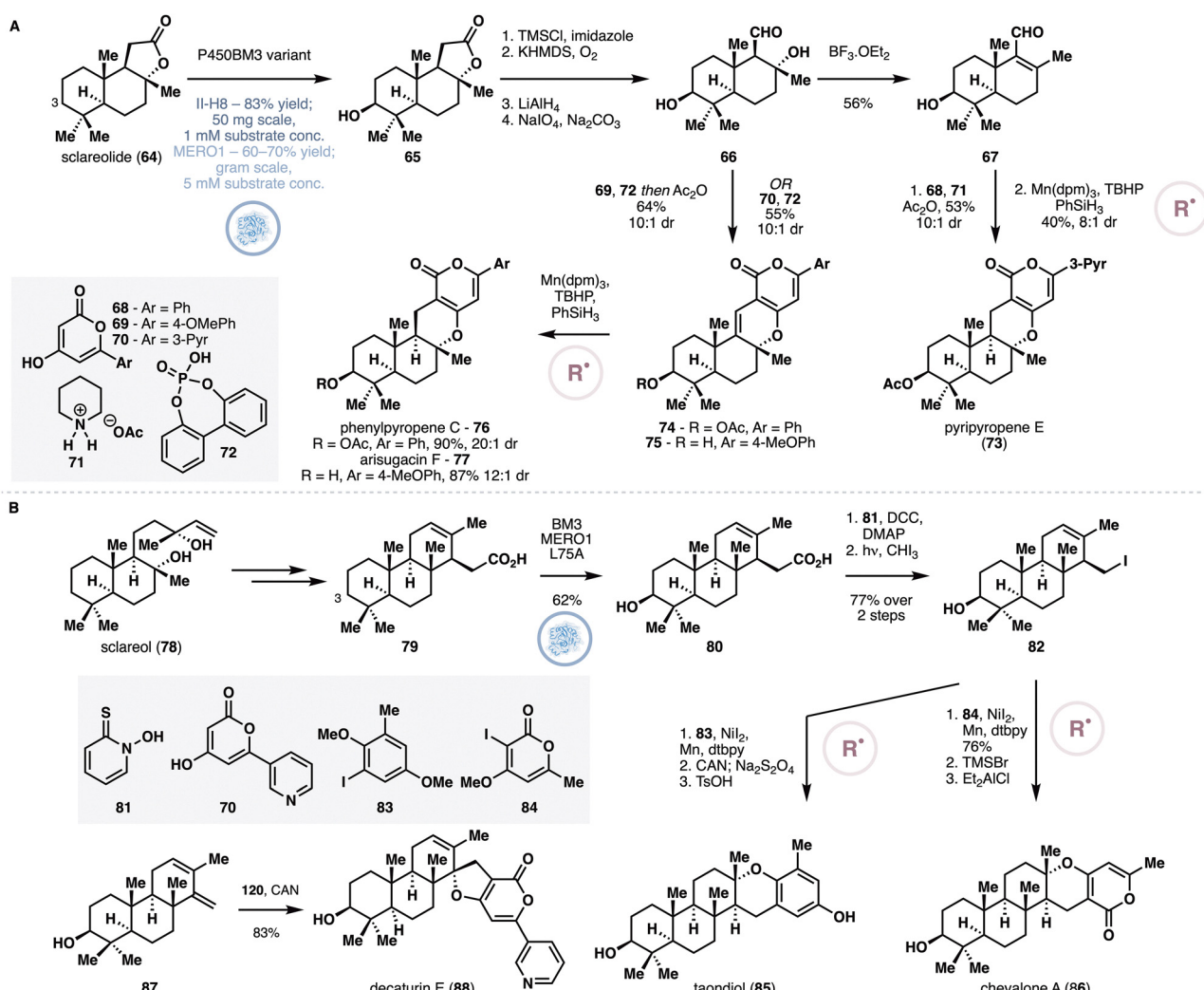


Fig. 7 (A) Chemoenzymatic synthesis of  $\alpha$ -pyrone meroterpenoids from sclareolide by Renata and co-workers featuring enzymatic oxidation at C3 and MHAT-based alkene reduction. (B) Chemoenzymatic synthesis of taondiol, chevalone A and decaturin E from sclareol by Renata and co-workers featuring enzymatic oxidation of **79** at C3.



proceeded with excellent stereo- and chemoselectivity to complete the synthesis of five different  $\alpha$ -pyrone meroterpenoids.

The Renata group further extended this blueprint to the synthesis of several oxidized meroditerpenoids from sclareol (78, Fig. 7B). Firstly, sclareol was converted to acid 79 through a five-step route featuring a radical-based intramolecular Giese addition<sup>52</sup> and lactone opening. All of the intermediates in this sequence were tested for hydroxylation with the aforementioned alanine-scanning library, which led to the discovery that 79 could be efficiently oxidized at its C3 carbon by variant MERO1 L75A, proceeding with 62% isolated yield on gram scale. The carboxylic acid moiety of 80 was used as a chemical handle to generate further structural complexity and complete the synthesis of four meroditerpenoid targets. Conversion of 80 to the corresponding iodide (82) set the stage for subsequent nickel cross coupling,<sup>53</sup> which delivered taondiol (85) and chevalone A (86) after routine deprotections. Alternatively, diene 87, obtained *via* elimination of 82, was subjected to a formal [3+2] coupling<sup>54</sup> to furnish decaturin E (88) and stypodiol.

### 3.2. Chemoenzymatic synthesis of gedunin

Having developed a scalable biocatalytic platform for selective C3 oxidation of sclareolide and related molecules, the Renata group in 2022 reported a convergent chemoenzymatic synthesis of deoxygedunin and gedunin (89),<sup>55</sup> two limonoids that have been reported to inhibit HSP90 and display antimalarial and neuroprotective properties (Fig. 8). With synthetic modularity in mind, the researchers conceived a fragment coupling with enone 91 for the synthesis, which could be obtained from sclareolide through MeLi addition, Baeyer–Villiger oxidation, C8–OH dehydration, ozonolysis and acetate elimination. Screening of a small panel of P450BM3 library revealed that variant MERO1 L437A was able to oxidize 91 at its C3 carbon with minimal side product arising from alkene epoxidation. Towards iodide 93, furfuryl alcohol (94) was combined with isoprene monoxide (95) under Krische's hydrogen auto-transfer

conditions,<sup>56</sup> which constructed the key C13 quaternary center with high diastereo- and enantioselectivity. Acylation of the secondary alcohol was followed by ring-closing metathesis to provide the corresponding unsaturated lactone. Finally, routine conversion of the primary alcohol to iodide generated 93. Fragments 92 and 93 were coupled under Luche's conditions,<sup>57</sup> and the resulting product was subjected to Wittig olefination with MePPh<sub>3</sub>Br. After DMP oxidation of the C3–OH and allylic oxidation at C7, an MHAT-based Giese coupling<sup>52</sup> furnished the tetracyclic framework of gedunin. Functional group manipulations consisting of Saegusa oxidation and acetylation at C7 completed the synthesis of deoxygedunin, which was converted to gedunin (89) through epoxidation with *m*CPBA.

### 3.3. Chemoenzymatic synthesis of drimane meroterpenoids *via* enzymatic building block production and enzymatic oxidation

Contemporaneous to the case study outline in Section 2.6, the Xiang group developed a chemoenzymatic approach to drimane meroterpenoids (Fig. 9) that combines heterologous production of drimenol, enzymatic hydroxylation and radical cross-couplings.<sup>58</sup> Using the authors' aforementioned system for introducing the MVA pathway in *E. coli*, the product titers of four drimenol synthases<sup>59</sup> were investigated. Among the four, DrtB demonstrated the highest activity, displaying a titer of 1.5 g L<sup>-1</sup> for the production of 49. Further metabolic engineering of the pathway improved the titer to 2.1 g L<sup>-1</sup>, providing ample material supply of 49 for the chemoenzymatic synthesis. Oxidation of 49 was initially investigated with P450BM3 F87A, which was capable of forming the desired C3 hydroxylated compound (99) as the main product. Further engineering led to variant P450BM3 L75A F87I, which delivered the desired product in 68% isolated yield on preparative scale. Appel reaction on 49 provided the corresponding primary bromide (101), which was subjected to radical cross-couplings<sup>60</sup> with a variety of aryl iodide partners. Similar to the approach outlined

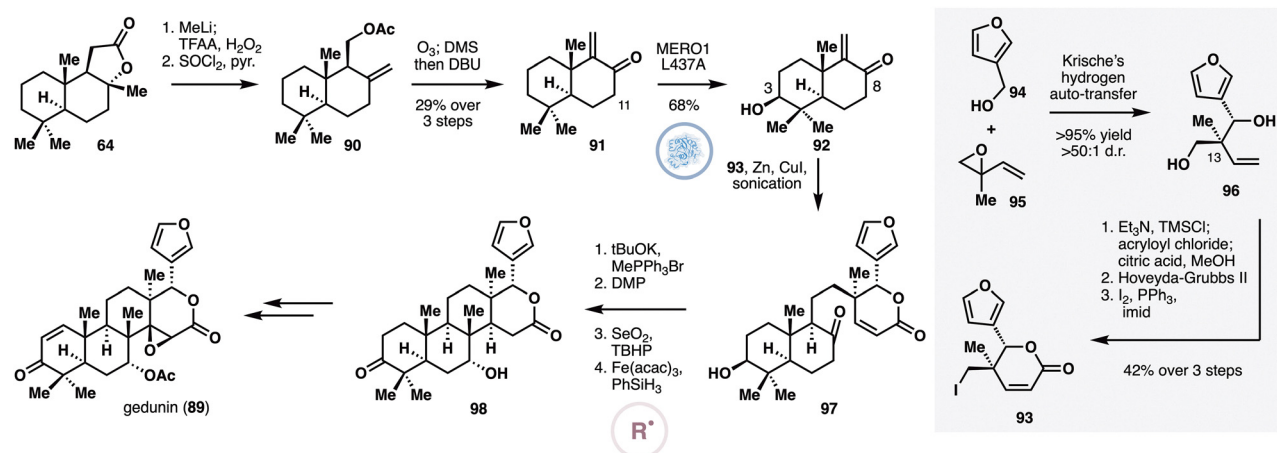


Fig. 8 Chemoenzymatic synthesis of gedunin by Renata and co-workers featuring site-selective enzymatic oxidation of 91 with P450BM3 variant MERO1 L437A and intramolecular Giese addition.



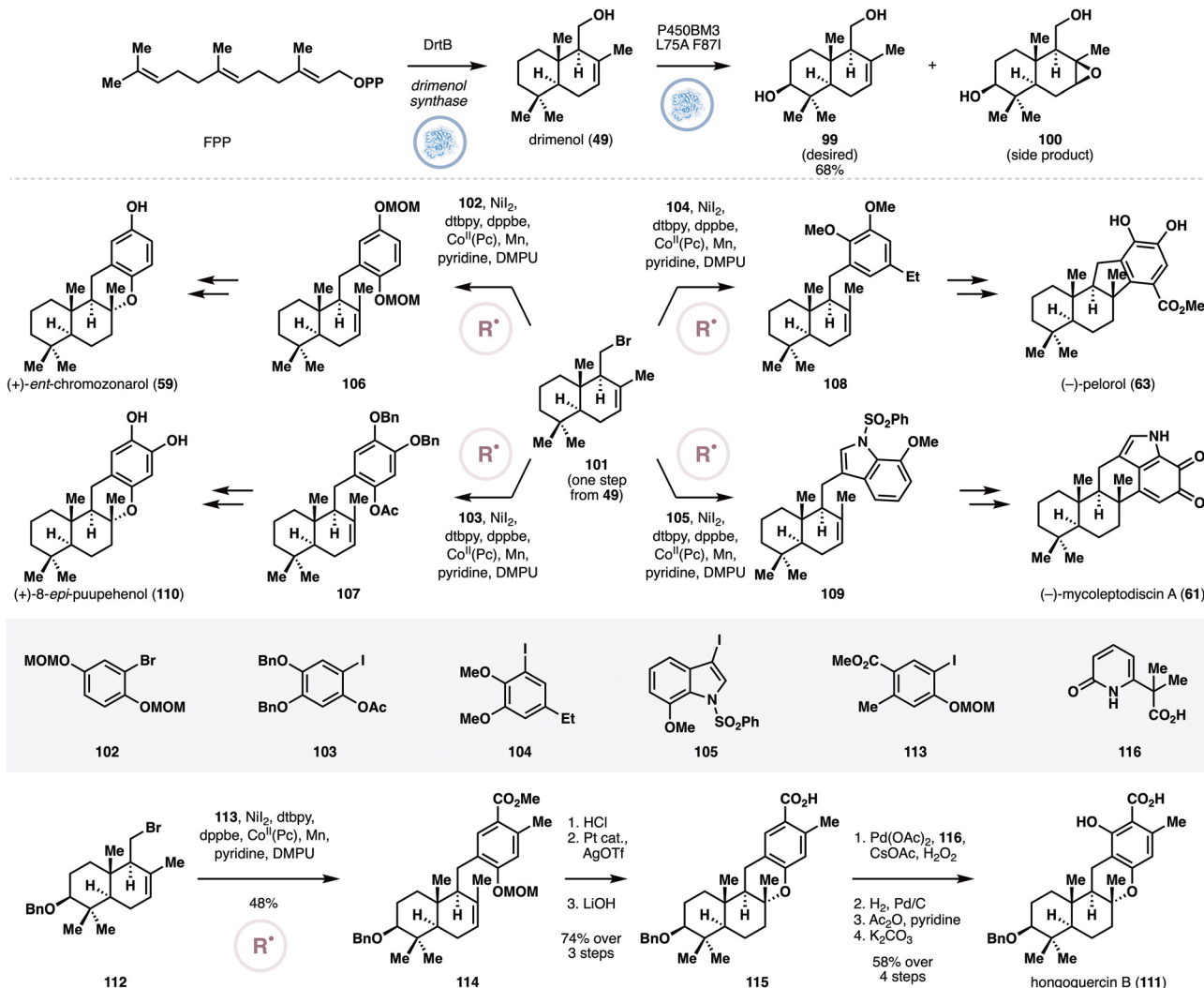


Fig. 9 Chemoenzymatic synthesis of drimane meroterpenoids by Xiang and co-workers via heterologous production of drimenol, its site-selective oxidation with P450BM3 L75A F87I and radical cross-couplings.

in Section 2.6, this route eventually completed the synthesis of *ent*-chromazonarol (59), 8-*epi*-puupehenol (110), pelorol (63) and mycoleptodiscin A (61). The same cross-coupling sequence could also be applied for the synthesis of hongoquercin B (111) *via* 112, which was prepared from 99 through a four-step sequence. Nickel-mediated cross-coupling of 112 and 113 was followed by MOM deprotection, pyran formation and ester hydrolysis to generate 115. The phenolic alcohol was then introduced *via* palladium-catalyzed C–H oxidation using Yu's protocol.<sup>61</sup> It should be noted that the authors resorted to this sequence as attempts to effect cross-coupling with the fully-elaborated aryl fragment was unsuccessful. With the general core structure constructed, three additional steps completed the synthesis of hongoquercin B (111).

### 3.4. Divergent chemoenzymatic synthesis of fusicoccane diterpenoids

The fusicocanes are fungal diterpenoids bearing a characteristic 5/8/5-tricyclic ring system.<sup>62</sup> Within the family, cotylenin A

and fusicoccin A are often regarded as the flagship members, as they were one of the firsts to be discovered and were noted to act as modulators of 14-3-3 protein–protein interactions.<sup>63</sup> More recently, additional family members that contain rearranged tricyclic skeletons have also been isolated, but their biological activities have not been profiled in detail. The Renata group sought to develop a modular chemoenzymatic strategy to target a wide range of family members, including those with rearranged skeletons.<sup>64</sup> Their design involves the chemical synthesis of a minimally oxidized 5/8/5-tricyclic intermediate, which would then be subjected to a series of chemoenzymatic oxidations. One of the key oxidations in the design hinges on prior biosynthetic studies by Dairi and Oikawa,<sup>65</sup> which identified the involvement of the NHDs BscD and Bsc9 in the C3 oxidation of compound 117 (Fig. 10). It was known that the reaction is accompanied by the formation of an unwanted shunt product (119) and at the outset, the researchers proposed that this issue could be addressable to additional screening and enzyme engineering.



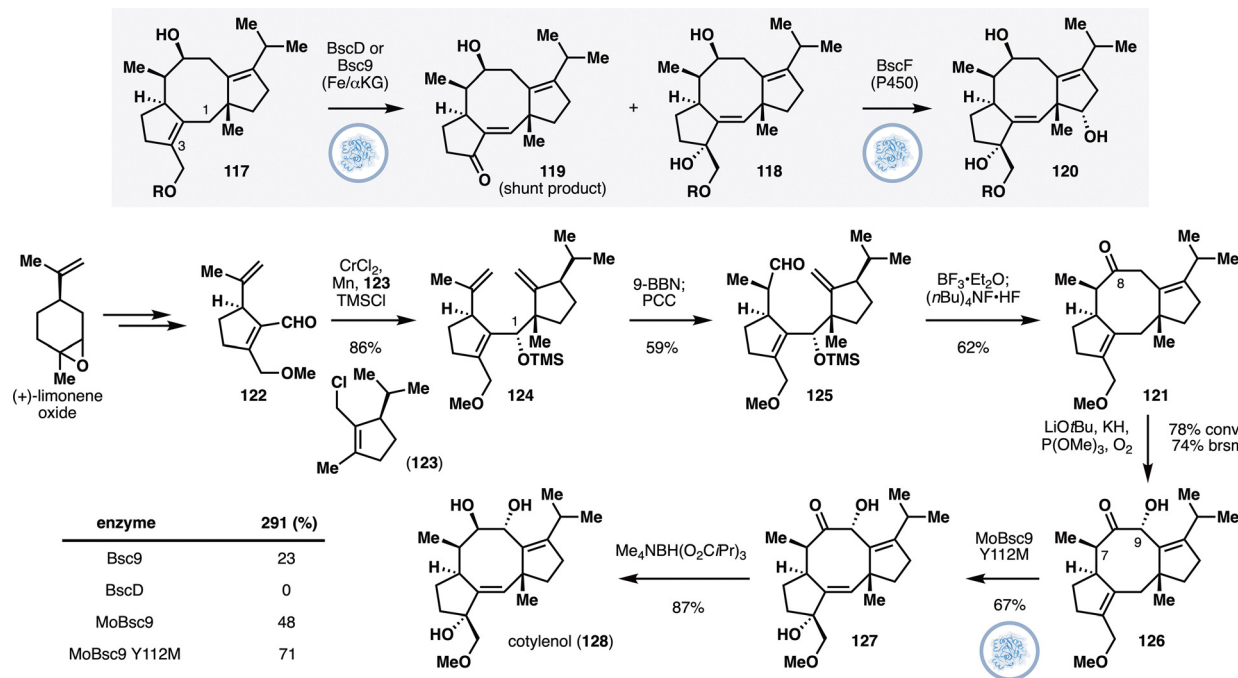


Fig. 10 Chemoenzymatic synthesis of cotylenol by Jiang and Renata featuring C3 oxidation of **126** with engineered MoBsc9.

In a departure from the native biosynthetic pathway, the researchers targeted ketone **121** as their key synthetic intermediate. A fragment coupling strategy was developed to access this ketone featuring the a Nozaki–Hiyama–Kishi coupling<sup>66</sup> between two cyclopentane units (**122** and **123**), which in turn were prepared from (+)-limonene oxide and (–)-limonene. A one-pot hydroboration/PCC oxidation delivered aldehyde **125**, which was serendipitously found to undergo a Prins cyclization with a transannular hydride shift to provide the desired ketone precursor for subsequent oxidations. Rubottom oxidation of this ketone installed the C9 alcohol and set the stage for subsequent investigation with BscD and Bsc9. While Bsc9 generated the desired oxidation product, significant formation of the undesired shunt product (*cf.* compound **119**) was also observed. To address this issue, the researchers performed Genome Neighborhood Network analysis<sup>67</sup> to pick several homologs of Bsc9 for further reaction with **126**. Among the homologs, MoBsc9 from *M. oryzae* offered improved reaction conversion and superior product distribution. Further active site engineering of MoBsc9 identified mutation Y112M that further improved the reaction conversion and product ratio, allowing the desired product (**127**) to be obtained in 67% isolated yield on 30 mg scale reaction. Finally, the conversion of **127** to cotylenol (**128**) was conducted following a protocol previously developed by Nakada and co-workers.<sup>68</sup>

Through a similar directed evolution campaign, mutations L110A and Y112R on MoBsc9 were discovered to improve the chemoselectivity of reaction with alcohol **129** (Fig. 11), delivering brassicicene I (**130**) in 64% isolated yield on 130 mg scale. Brassicicene I was further found to undergo selective C13 hydroxylation with P450BM3 variant MERO1 L75A in 78% yield. On the other hand, palladium-catalyzed allylic oxidation<sup>69</sup>

formed the enone product, completing the synthesis of brassicicene A (**131**), which was converted to brassicicene R (**132**) through routine Rubottom oxidation. The allylic alcohol from MERO1 L75A oxidation could be dehydrated to the resulting cyclopentadiene (**134**), which was then subjected to  $^1\text{O}_2$  Diels–Alder and Kornblum–Delamare rearrangement to afford brassicicene L (**136**). Towards the rearranged fusicocanes, a partially protected derivative of brassicicene R (**137**) was submitted to a chemoselective Wagner–Meerwein shift in the presence of  $\text{Tf}_2\text{O}$  and pyridine. After silyl ether deprotection, brassicicene K (**138**) was obtained.<sup>70</sup> Selective hydrogenation of the *exo* methylene of **138** generated brassicicene C (**139**), which was reduced with DIBAL reduction to afford brassicicene H (**140**). Alternatively, **141** could also be subjected to Mukaiyama hydroperoxidation<sup>71</sup> and deprotection to deliver brassicicene J (**142**), or Mukaiyama hydration and deprotection to provide brassicicene F (**143**). In total ten fusicocane natural products were prepared using this chemoenzymatic approach.

### 3.5. Chemoenzymatic synthesis of non-terpenoid targets

**3.5.1. Renata's synthesis of podophyllotoxin and related aryltetralin lignans.** Podophyllotoxin (**144**) is an aryltetralin lignan that can serve as a highly potent microtubule depolymerizing agent.<sup>72</sup> This property has led to semisynthetic efforts to optimize the anticancer properties of the molecule, culminating in the invention of two derivatives, etoposide and teniposide, as chemotherapy agents. In 2019,<sup>73</sup> the Renata group reported an asymmetric chemoenzymatic approach to podophyllotoxin and additional aryltetralin lignans by drawing inspiration from a prior biosynthetic study by Lau and Sattely (Fig. 12A),<sup>74</sup> which suggested the involvement of a late-stage oxidative cyclization from yatein (**145**) by an NHD, 2-ODD-PH,



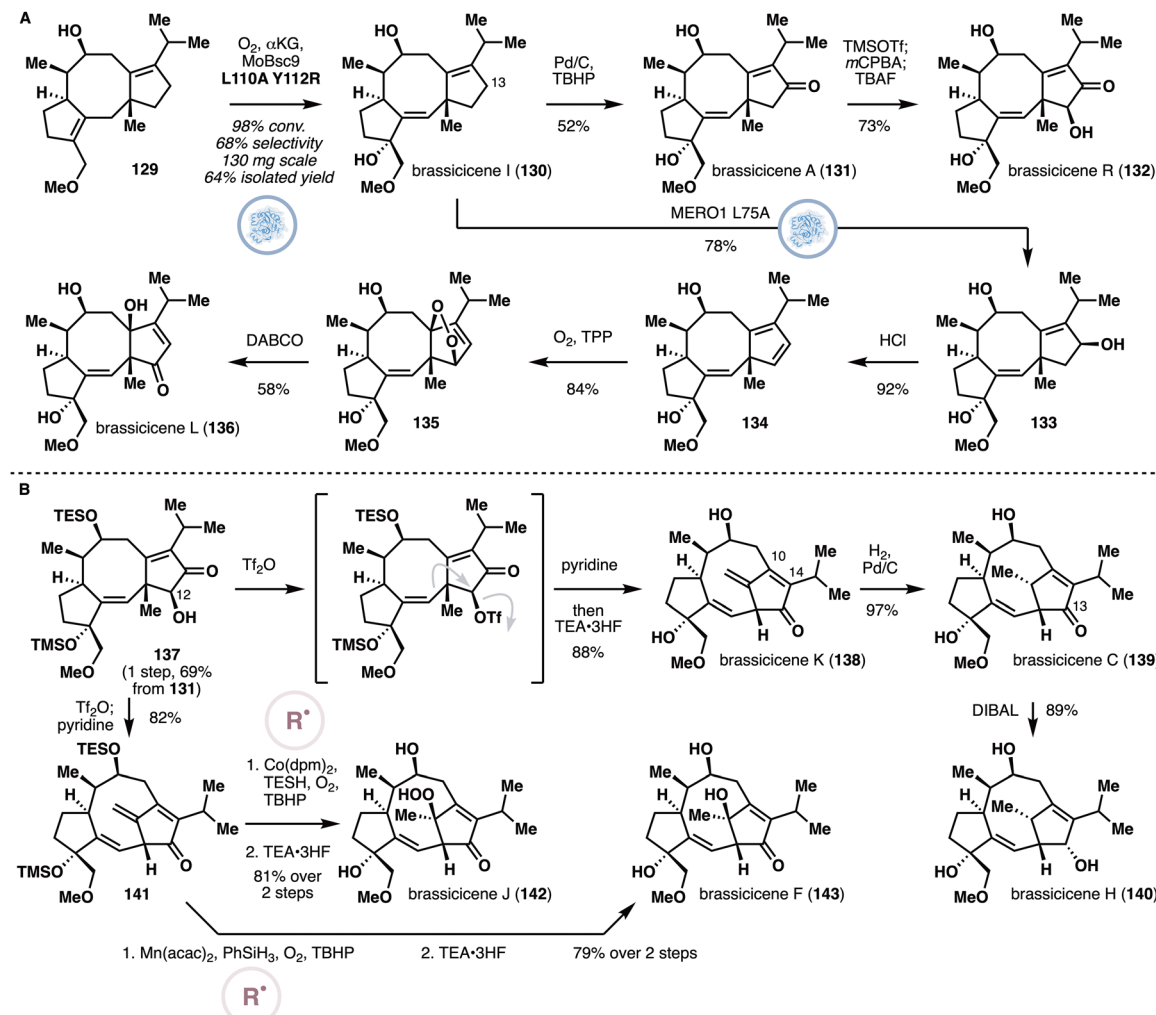


Fig. 11 Chemoenzymatic synthesis of oxidized and rearranged fusicocanes by Jiang and Renata. (A) Synthesis of brassicicenes A, I, L and R. (B) Synthesis of brassicicene C, F, J, and H.

in the biogenesis of podophyllotoxin. The general blueprint of their approach is to develop a concise chemical access to yatein, and subject it to chemoenzymatic redox adjustments to arrive at podophyllotoxin. Towards yatein, the authors enlisted the use of oxidative enolate coupling methodology developed by Baran,<sup>75</sup> which presumably proceeds through single electron oxidation, followed by radical–radical coupling. Thus, 147 and 148 were enolized with LDA and treated *in situ* with a Cu<sup>II</sup> salt to furnish the desired dicarbonyl product. Selective monoreduction with LiBH<sub>4</sub> and equilibration of the initial diastereomeric mixture with DBU generated yatein as a single diastereomer in 51% overall yield. Oxidative cyclization in the presence of 2-ODD-PH generated the desired tetracycle in 95% yield. Finally, benzylic oxidation of 146 with CrO<sub>3</sub> and 3,5-dimethylpyrazole, followed by ketone reduction with L-selectride completed the synthesis of podophyllotoxin. In this work, the authors also conducted a systematic substrate–activity relationship profiling of 2-ODD-PH, which resulted in the synthesis of five additional aryltetralin lignans, including the natural products polygamain (149), morelensin (150), austrobailignan 1 (151) and hernandin

(152). It should be noted that the Fuchs and Kroutil group<sup>76</sup> contemporaneously reported a complementary approach to podophyllotoxin by combining a biocatalytic kinetic resolution of a dibenzylbutyrolactone precursor and oxidative cyclization with 2-ODD-PH.

**3.5.2. Li's synthesis of prostaglandins.** Prostaglandins are a group of lipid-derived, hormone-like substances that play key regulatory roles in various metabolic functions.<sup>77</sup> In light of this property, there has been a lot of interests in creating prostaglandin derivatives with improved chemical stability and reduced side effects. To date, more than 20 prostaglandin-derived drugs have been clinically approved and numerous *de novo* syntheses have also been reported. A well-known strategy in these syntheses involves the use of Corey lactone,<sup>78</sup> which contains a primary alcohol for a variety of derivatizations through two-electron chemistry. The Li group sought to complement this approach by developing a bromide counterpart of the lactone, which would be amenable to use in radical cross-couplings.<sup>79</sup>

Toward the above goal, the authors explored two sequences to prepare the target bicyclic (Fig. 12B). Firstly, *meso*-diol 153

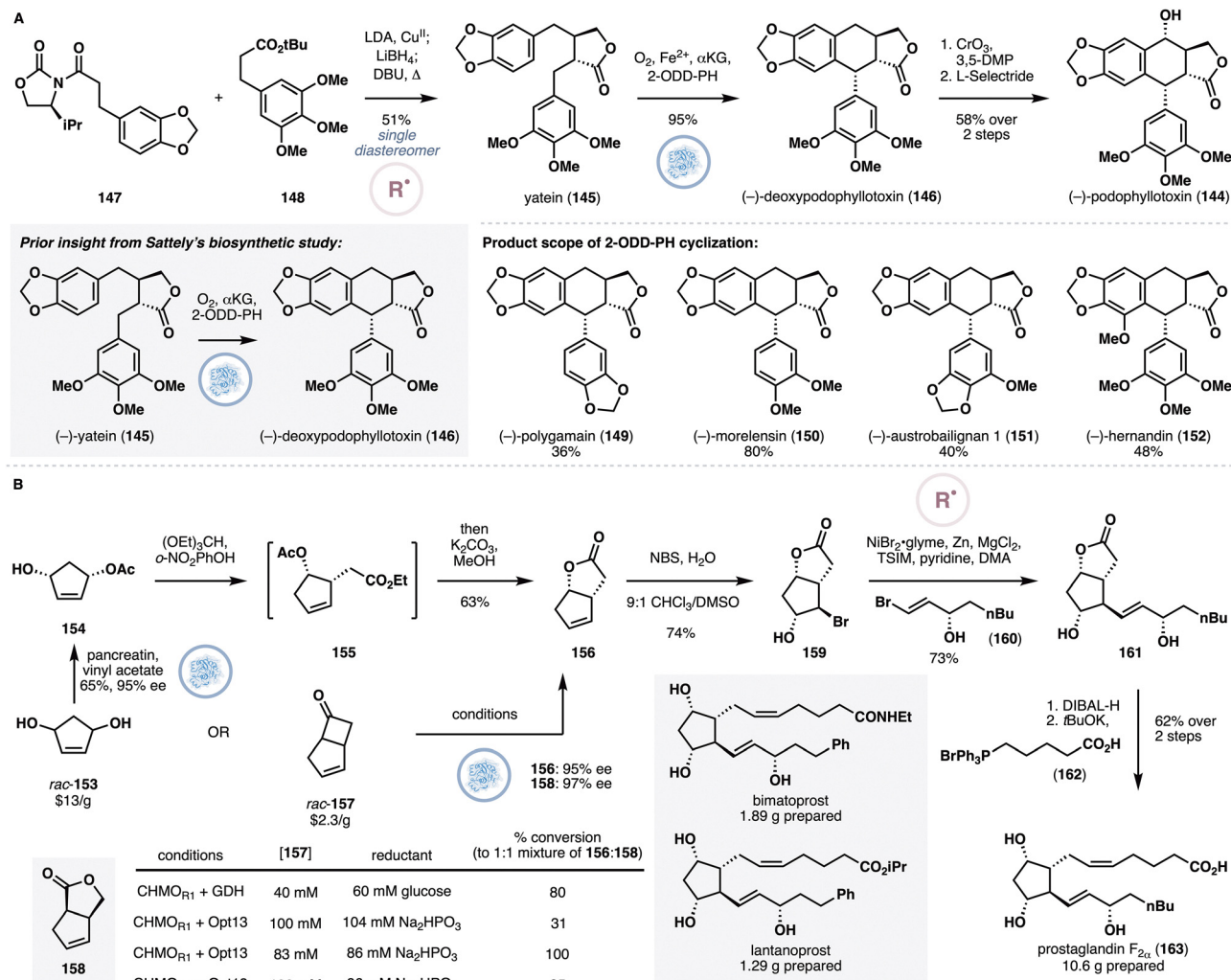


Fig. 12 (A) Chemoenzymatic synthesis of podophyllotoxin by Renata and co-workers via oxidative enolate coupling and enzymatic oxidative cyclization with 2-ODD-PH. (B) Chemoenzymatic synthesis of prostaglandins by Li and co-workers.

was desymmetrized through lipase-mediated esterification,<sup>80</sup> and then subjected to a Johnson–Claisen rearrangement and lactonization. This sequence was eventually abandoned in favor of an alternative one that commenced from a cheaper starting material, cyclobutanone 157. Enzymatic Baeyer–Villiger<sup>81</sup> of 157 in the presence of CHMO<sub>rhodo1</sub> and Opt13 for NADPH regeneration afforded lactones 156 and 158 in 95% and 97% ee respectively. Remarkably, this reaction could be conducted at 83 mM substrate concentration, affording >100 g of 156 throughout the synthetic campaign. After extensive optimization, 156 could be converted to the desired bromohydrin diastereomer 159, which set the stage for the key radical cross-coupling. Initial foray into this reaction led to significant formation of an undesired epoxide byproduct, in addition to the desired product 161. This issue was solved by the addition of trimethylsilylimidazole for *in situ* alcohol protection. With this modification, the desired cross-coupling proceeded smoothly either with one equivalent of pyridine or 0.15 equivalent of a bidentate bipyridine ligand. A range of vinyl and aryl bromides were found to be suitable coupling partners, affording at least

60% yield. Starting from cross-coupling product 161, two uneventful steps, namely lactone reduction and aldehyde homologation, led to prostaglandin F<sub>2α</sub> (163). Using a similar sequence, additional prostaglandins, such as bimatoprost, fluprostenol, cloprostenol and lantanoprost, were prepared. As a testament to the robustness of the route, each of these molecules was obtained in more than 1 g quantity.

**3.5.3. Chemoenzymatic functionalization of piperidine carboxylic acid isomers.** Piperidine is one of the most common heterocycles found in clinically-approved drugs and pharmaceutical leads. Especially valuable in this area are chiral piperidines that contain multiple substitutions. A recent survey suggests that di- and trisubstituted piperidines cumulatively make up for approximately 71% of piperidine-based drugs.<sup>82</sup> The ubiquity of multisubstituted piperidines has spurred the development of various methods for their construction. Common approaches<sup>83</sup> in this area include *de novo* ring synthesis *via* intramolecular cyclization and dearomatic functionalization of pyridines. However, *de novo* ring construction often requires lengthy substrate preparation and asymmetric dearomatic

functionalization still requires chiral auxiliary and is often beset by regioselectivity challenges. Thus, there is still an unmet demand for an efficient synthesis of densely-functionalized, chiral piperidines with diverse substitution patterns.

A recent collaborative work<sup>84</sup> from the Baran and Renata groups developed a chemoenzymatic approach to complex piperidines by relying on site-selective oxidations of several piperidine carboxylic acid regioisomers, followed by radical cross-couplings for rapid elaboration. The researchers noted several early reports on oxidizing L-pipecolic acid (L-Pip, 164, Fig. 13A) at its C2, C3 and C4 positions with the NHDs GetF (C2),<sup>85</sup> FoPip4H (C3)<sup>86</sup> and *trans*-P4H/P4H810 (*trans/cis* C4)<sup>87</sup> respectively and embarked on an extensive screening campaign to systematically optimize the performance of the enzymes for large-scale biotransformations. Eventually, a set of conditions was identified for each enzyme that allows gram-scale access to building blocks 165–168 on gram scale. In addition, the researchers also sought to identify a biocatalytic system for the oxidation of nipecotic acid (D-Nip, 169). Screening of a small pool of NHDs identified ectoine 5-hydroxylase<sup>88</sup> from *S. alaskensis* as a viable biocatalyst for the C4 hydroxylation of D-Nip, which was further optimized through evaluation of various reaction parameters to eventually afford 100% conversion on 15 mM substrate loading. Cumulatively, five key fragments (171–175) were successfully prepared in gram or near-gram quantities from the enzymatic oxidations after simple Boc protection.

Starting from 171–175, a number of synthetic targets, including alkaloidal natural products and active pharmaceutical ingredients,

were successfully obtained through the use of Ni-based cross couplings that rely either on the free carboxylic acid or the newly-introduced alcohol as cross-coupling handle. To specifically highlight in the context of natural product synthesis (Fig. 13B), 171, obtained *via* biocatalytic oxidation with GetF, was first converted to its NHPI ester counterpart and submitted to an electrochemical decarboxylative cross-coupling<sup>89</sup> with vinyl iodide 176 to furnish allyl alcohol 177 in 49% yield and 19:1 dr. The primary alcohol of 177 was selectively converted to the corresponding bromide under standard Appel conditions and removal of the Boc group led to simultaneous cyclization to afford a penultimate bicyclic intermediate. Finally, alkene dihydroxylation in the presence of OsO<sub>4</sub> completed the synthesis of (–)-swainsonine (178). Conversely, 172, obtained *via* biocatalytic oxidation with FoPip4H, was combined with vinyl bromide 179 under the same electrochemical decarboxylative cross-coupling conditions. Following Boc group removal with TFA, the *Streptomyces* alkaloid SS20846A (180) was obtained.

**3.5.4. Baran's synthesis of saxitoxin.** Saxitoxin (181) is a well-known parasitic shellfish toxin that exhibits lethal neurotoxicity by inhibiting voltage-gated sodium channels.<sup>90</sup> Its unusual structure, in combination with its potential use as anesthetics in pain treatment and management, has led to the development of many synthetic approaches to the natural product. Very recently, the Baran group, in collaboration with scientists from Merck, reported<sup>91</sup> a concise chemoenzymatic access to 181 and several congeners that features the use of radical cross-coupling and biocatalytic oxidation as its key steps.

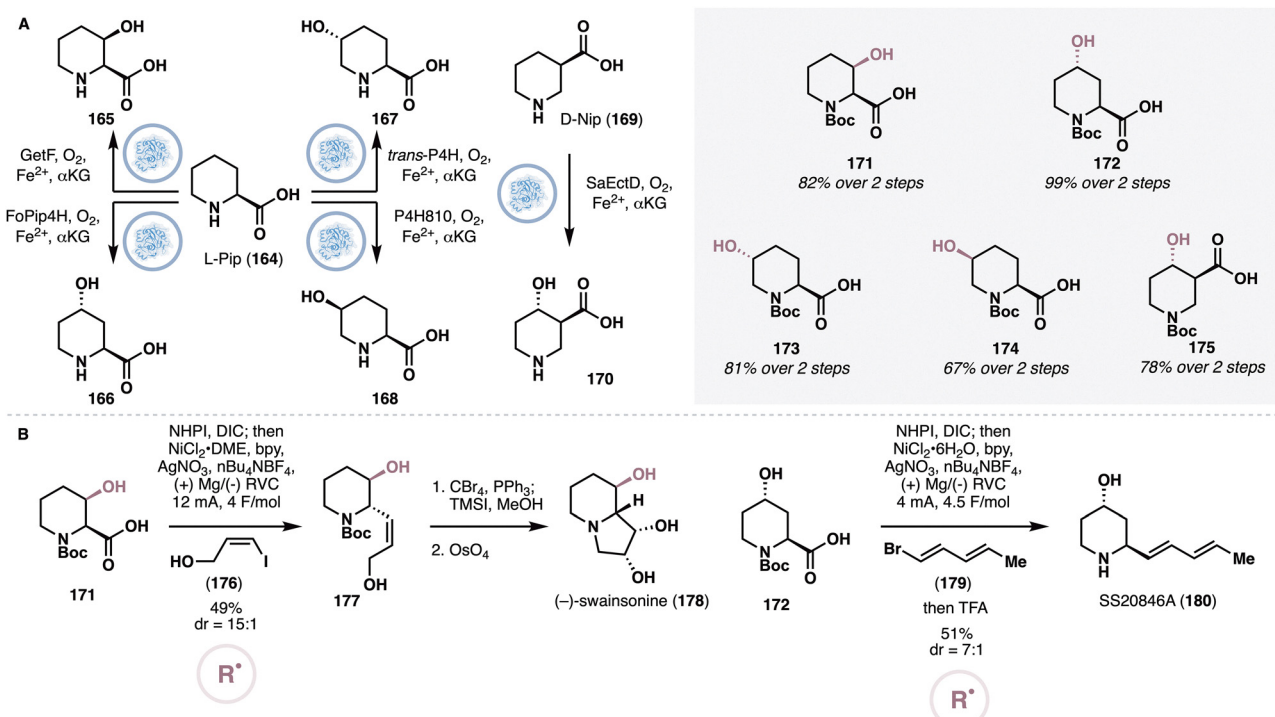


Fig. 13 (A) Divergent enzymatic oxidation of L-pipecolic acid to 165–168 and enzymatic oxidation of D-nipecotic acid to 170. (B) Baran and Renata's approach to swainsonine and SS20846A via electrochemical cross-couplings of 171 and 172 respectively.



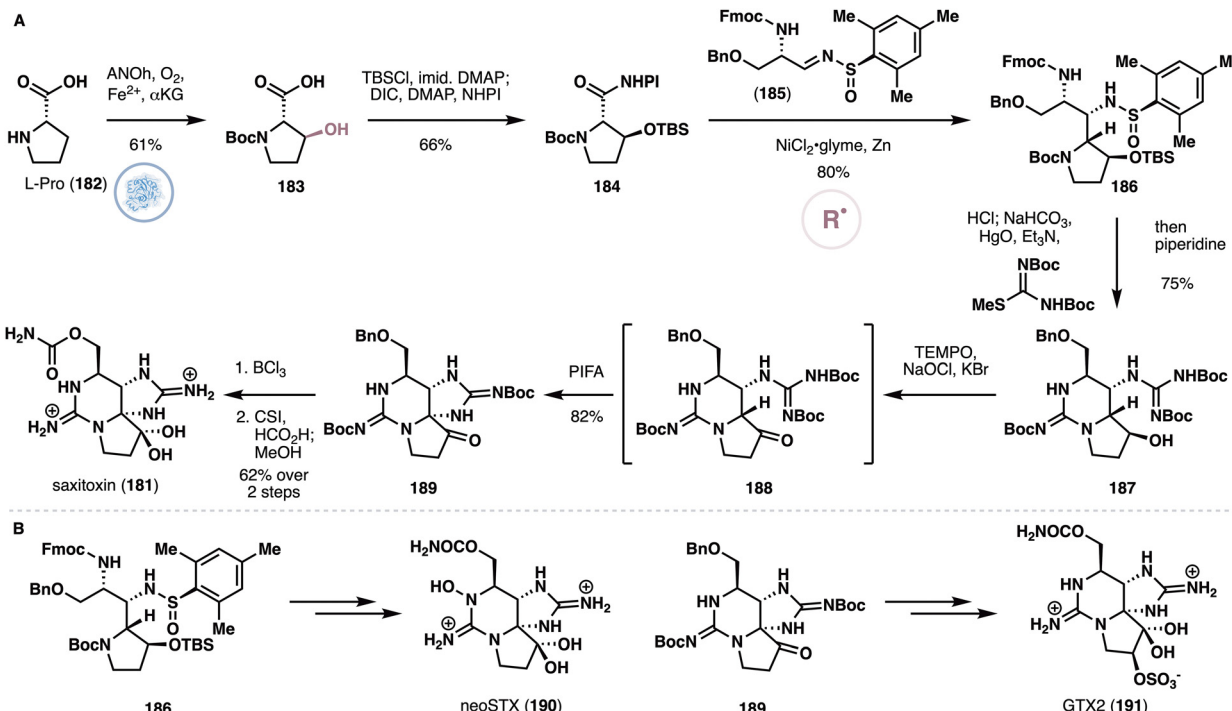


Fig. 14 (A) Baran's synthesis of saxitoxin featuring enzymatic oxidation of L-proline with ANOH and radical coupling with sulfinimine **185**. (B) Extension of the approach to the synthesis of neosaxitoxin and gonyautoxin 2.

The researchers posited that the substituted pyrrolidine motif on **181** could potentially arise from a hydroxylated derivative of L-proline (**182**). However, additional stereochemical considerations suggested the need for *trans*-3-hydroxyproline as starting material. Due to its prohibitive cost, a variety of approaches were investigated for its large-scale synthesis, culminating in the development of a biocatalytic oxidation route. While oxidation of L-proline to its *trans*-3-hydroxy counterpart has never been reported previously, the team found that a previously uncharacterized fungal NHD named ANOH was able to generate a 1.2 : 1.0 mixture of the *trans*-3 and *trans*-4 isomers from L-proline (Fig. 14). Further engineering of this enzyme resulted in a variant called CDX-090, which exclusively produces *trans*-3-hydroxyproline with exceptionally high reaction titer (substrate loading of  $>30\text{ g L}^{-1}$ ).

Following Boc and TBS protection, the resulting intermediate was submitted to a decarboxylative coupling<sup>92</sup> with sulfinimine **185** to provide **186** as a single diastereomer in 80% yield. The team noted that the more conventional Mannich disconnection was also attempted but was met with no success. A telescoped process was next developed featuring Boc deprotection, double guanidylation and intramolecular ring closure to generate bicyclic **187** in 75% yield. After oxidation under Anelli conditions, the resulting ketone was immediately treated with PIFA *in situ* to effect an oxidative C–N bond formation a to the ketone, thereby forging the signature tricyclic ring system of **181**. Here, the researchers also examined alternative C–H amination or oxidation conditions for forge the C4–N9 bond, but all these conditions did not lead to any promising results. To complete the synthesis of **181**, global deprotection with BCl<sub>3</sub> and carbamoylation of the primary alcohol were performed,

resulting in a seven-step synthesis of **181** (longest linear sequence). Using the initial synthesis of **181** as a template, the authors further showed that intermediates **186** and **189** could be used as starting points for accessing a number of congeners (Fig. 14B), including neosaxitoxin (neoSTX, **190**) and gonyautoxin 2 (GTX2, **191**).

## 4. Conclusions

This review outlines numerous case studies wherein enzymatic and radical reactions were combined in a strategic fashion to efficiently synthesize complex natural products. For example, the use of terpene cyclases enables the formation of multiple C–C bonds and unique ring systems from simple, acyclic precursors in one step. In contrast, chemical synthesis of the analogous carbocycles usually requires multi-step sequences that also need to take into account various stereoelectronic and thermodynamic factors. When combined with the unique reactivity profile and the high functional group compatibility of modern radical reactions, it is perhaps not a surprise that the resulting hybrid approach would result in unparalleled synthetic efficiency. Similar benefits in synthetic economy can also be obtained by combining modern radical reactions for skeletal construction and enzymatic tailoring with oxygenases as modern radical reactions offer the ability to make unconventional bond disconnections and oxygenases are capable of performing selective oxidations and functionalizations that are otherwise challenging to perform with traditional chemical methods. Despite these advantages, several

challenges—especially in enzymatic reaction development—still exist and need to be addressed to further expand the generality of the chemoenzymatic strategies outlined above. Not all terpene cyclases are capable of producing the desired carbocyclic scaffolds in high titers and extensive metabolic and protein engineering may be needed to boost the titers to levels that are appropriate for material supply in multi-step syntheses. It is also generally difficult to predict the substrate promiscuity of a given enzyme at present and in the context of enzymatic oxidation specifically, we still do not have sufficient capability to predict the site-selectivity of a given oxygenase when applied on substrates whose structure differ substantially from what have been reported previously. As such, enzymatic oxidations on such scaffolds may require extensive screening for the identification of the right enzyme(s). Presently, such screening can be done with “brute force” chromatographic methods, but incorporation of more modern platforms such as droplet microfluidic<sup>93</sup> for higher screening throughput, or deep learning models for activity prediction,<sup>94</sup> could alleviate the screening burden. As can be seen in the case studies presented, there has been a lot of emphasis on the use of terpene cyclases and oxygenases in current approaches in chemoenzymatic synthesis of natural products. However, this is not to say that other enzyme families are less applicable. In fact, there is a lot of untapped opportunities in the use of other enzyme families in this author’s view. The recent surge in the development of new-to-nature biocatalytic reactions, especially in the area of radical reactions,<sup>95</sup> is particularly exciting in this regard, as they open up a gamut of possibilities for even more inventive reaction combinations in chemoenzymatic total synthesis. Progress in chemoenzymatic synthesis has also been slowed by limited avenues for knowledge dissemination and accessibility to resources—for example: a lack of searchable database for biocatalytic reactions and a lack of familiarity with the general concepts and the technical aspects of biocatalysis among practitioners of organic chemistry—, and more concerted educational efforts,<sup>96</sup> including the introduction of biocatalysis/enzyme catalysis in formal curricula and the development of biocatalysis-focused workshops, could help accelerate progress. These challenges are by no means insurmountable and on the whole, the increasing number of chemoenzymatic total synthesis that features a combination of enzymatic and radical reactions in the past decade heralds a rosy long-term prospect. Thus, we anticipate that the field will see exponential advancements in the future in accord with new technological advances in both areas.

## Conflicts of interest

There are no conflicts to declare.

## Data availability

No primary research results have been included and no new data were generated or analyzed as part of this review.

## Acknowledgements

Our research in this area is supported by the National Institutes of Health (grant GM128895) and the National Science Foundation (CAREER award #1945468).

## References

- 1 (a) C. K. Prier, D. A. Rankic and D. W. C. MacMillan, Visible light photoredox catalysis with transition metal complexes: Applications in organic synthesis, *Chem. Rev.*, 2013, **113**, 5322; (b) N. A. Romero and D. A. Nicewicz, Organic photoredox catalysis, *Chem. Rev.*, 2016, **116**, 10075; (c) J. D. Bell and J. A. Murphy, Recent advances in visible light-activated radical coupling reactions triggered by (i) ruthenium, (ii) iridium and (iii) organic photoredox reagents, *Chem. Soc. Rev.*, 2021, **50**, 9540.
- 2 M. Yan, Y. Kawamata and P. S. Baran, Synthetic organic electrochemical methods since 2000: On the verge of a renaissance, *Chem. Soc. Rev.*, 2017, **117**, 13230.
- 3 (a) H. Yi, G. Zhang, H. Wang, Z. Huang, J. Wang, A. K. Singh and A. Lei, Recent advances in radical C–H activation/radical cross-coupling, *Chem. Rev.*, 2017, **117**, 9016; (b) J. Xie, H. Jin and A. S. K. Hashmi, The recent achievements of redox-neutral radical C–C cross-coupling enabled by visible-light, *Chem. Soc. Rev.*, 2017, **46**, 5193; (c) D. L. Golden, S.-E. Suh and S. S. Stahl, Radical C(sp<sup>3</sup>)-H functionalization and cross-coupling reactions, *Nat. Rev. Chem.*, 2022, **6**, 405; (d) A. Y. Chan, I. B. Perry, N. B. Bissonnette, B. F. Buksh, G. A. Edwards, L. I. Frye, O. L. Garry, M. N. Lavagnino, B. X. Li, Y. Liang, E. Mao, A. Millet, J. V. Oakley, N. L. Reed, H. A. Sakai, C. P. Seath and D. W. C. MacMillan, Metallaphotoredox: The merger of photoredox and transition metal catalysis, *Chem. Rev.*, 2022, **122**, 1485.
- 4 (a) S. A. Green, S. W. M. Crossley, J. L. M. Matos, S. Vasquez-Cespedes, S. L. Shevick and R. A. Shenvi, The high chemofidelity of metal-catalyzed hydrogen atom transfer, *Acc. Chem. Res.*, 2018, **51**, 2628; (b) S. L. Shevick, C. V. Wilson, S. Kotesova, D. Kim, P. L. Holland and R. A. Shenvi, Catalytic hydrogen atom transfer to alkenes: a roadmap for metal hydrides and radicals, *Chem. Sci.*, 2020, **11**, 12401; (c) J. Wu and Z. Ma, Metal-hydride hydrogen atom transfer (MHAT) reactions in natural product synthesis, *Org. Chem. Front.*, 2021, **8**, 7050.
- 5 J. M. Smith, S. J. Harwood and P. S. Baran, Radical retrosynthesis, *Acc. Chem. Res.*, 2018, **51**, 1807.
- 6 G. Laudadio, M. D. Palkowitz, T. E.-H. Ewing and P. S. Baran, Decarboxylative cross-coupling: a radical tool in medicinal chemistry, *ACS Med. Chem. Lett.*, 2022, **13**, 1413.
- 7 (a) N. J. Turner and E. O'Reilly, Biocatalytic retrosynthesis, *Nat. Chem. Biol.*, 2013, **9**, 285; (b) A. P. Green and N. J. Turner, Biocatalytic retrosynthesis: redesigning synthetic routes to high-value chemicals, *Perspect. Sci.*, 2016, **9**, 42; (c) R. O. M. A. de Souza, L. S. M. Miranda and U. T. A. Bornscheuer, retrosynthesis approach for biocatalysis in organic synthesis, *Chem. – Eur. J.*, 2017, **23**, 12040.



8 S. Chakrabarty, Y. Wang, J. C. Perkins and A. R. H. Narayan, Scalable biocatalytic C–H oxyfunctionalization reactions, *Chem. Soc. Rev.*, 2020, **49**, 8137.

9 (a) D. C. Miller, S. V. Athavale and F. H. Arnold, Combining chemistry and protein engineering for new-to-nature biocatalysis, *Nat. Synth.*, 2022, **1**, 18; (b) Y. Yang and F. H. Arnold, Navigating the unnatural reaction space: directed evolution of heme proteins for selective carbene and nitrene transfer, *Acc. Chem. Res.*, 2021, **54**, 1209; (c) C. K. Prier and F. H. Arnold, Chemomimetic biocatalysis: exploiting the synthetic potential of cofactor-dependent enzymes to create new catalysts, *J. Am. Chem. Soc.*, 2015, **137**, 13992; (d) H. Renata, Z. J. Wang and F. H. Arnold, Expanding the enzyme universe: accessing non-natural reactions by mechanism-guided directed evolution, *Angew. Chem., Int. Ed.*, 2015, **54**, 3351.

10 (a) T. Benkovics, *et al.*, Diverse catalytic reactions for the stereoselective synthesis of cyclic dinucleotide MK-1454, *J. Am. Chem. Soc.*, 2022, **144**, 5855; (b) J. A. McIntosh, *et al.*, A kinase-cGAS cascade to synthesize a therapeutic STING activator, *Nature*, 2022, **603**, 439; (c) M. A. Huffman, *et al.*, Design of an in vitro biocatalytic cascade for the manufacture of islatravir, *Science*, 2019, **366**, 1255; (d) A. Fryszkowska, *et al.*, A chemoenzymatic strategy for site-selective functionalization of native peptides and proteins, *Science*, 2022, **376**, 1321.

11 (a) R. Croteau, Biosynthesis and catabolism of monoterpenoids, *Chem. Rev.*, 1987, **87**, 929; (b) C. A. Lesburg, J. M. Caruthers, C. M. Paschall and D. W. Christianson, Managing and manipulating carbocations in biology: terpenoid cyclase structure and mechanism, *Curr. Opin. Struct. Biol.*, 1998, **8**, 695.

12 (a) D. W. Christianson, Structural and chemical biology of terpenoid cyclases, *Chem. Rev.*, 2017, **117**, 11570; (b) D. W. Christianson, Structural biology and chemistry of the terpenoid cyclases, *Chem. Rev.*, 2006, **106**, 3412; (c) P. Moosmann, F. Ecker, S. Leopold-Messer, J. K. B. Cahn, C. L. Dieterich, M. Groll and J. Piel, A monodomain class II terpene cyclase assembles complex isoprenoid scaffolds, *Nat. Chem.*, 2020, **12**, 968; (d) T. Hoshino and T. Sato, Squalene-hopene cyclase: catalytic mechanism and substrate recognition, *Chem. Commun.*, 2002, 291.

13 I. Buhaescu and H. Izzedine, Mevalonate pathway: a review of clinical and therapeutic implications, *ClinBiochem*, 2007, **40**, 575.

14 A. Banerjee and T. D. Sharkey, Methylerythritol 4-phosphate (MEP) pathway metabolic regulation, *Nat. Prod. Rep.*, 2014, **31**, 1043.

15 Y. Tu, The discovery of artemisinin (qinghaosu) and gifts from Chinese medicine, *Nat. Med.*, 2011, **17**, 1217.

16 C. J. Paddon and J. D. Keasling, Semi-synthetic artemisinin: a model for the use of synthetic biology in pharmaceutical development, *Nat. Rev. Microbiol.*, 2014, **12**, 355.

17 D.-K. Ro, *et al.*, Production of the antimalarial drug precursor artemisinic acid in engineered yeast, *Nature*, 2006, **440**, 940.

18 P. J. Westfall, *et al.*, Production of amorphadiene in yeast, and its conversion to dihydroartemisinic acid, precursor to the antimalarial agent, *Proc. Natl. Acad. Sci. U. S. A.*, 2012, **109**, 111.

19 C. J. Paddon, *et al.*, High-level semi-synthetic production of the potent antimalarial artemisinin, *Nature*, 2013, **496**, 528.

20 J. Turconi, *et al.*, Semisynthetic artemisinin, the chemical path to industrial production, *Org. Proc. Res. Dev.*, 2014, **18**, 417.

21 R. Ratnayake, D. Covell, T. T. Ransom, K. R. Gustafson and J. A. Beutler, Englerin A, a selective inhibitor of renal cancer cell growth, from *Phyllanthus engleri*, *Org. Lett.*, 2009, **11**, 57.

22 Y. Akbulut, *et al.*, (–)-Englerin A is a potent and selective activator of TRPC4 and TRPC5 calcium channels, *Angew. Chem., Int. Ed.*, 2015, **54**, 3787.

23 T. Siemon, *et al.*, Semisynthesis of plant-derived englerin A enabled by microbe engineering of guaia-6,10(14)-diene as building block, *J. Am. Chem. Soc.*, 2020, **142**, 2760.

24 I. Burkhardt, *et al.*, Mechanistic characterization of two sesquiterpene cyclases from the plant pathogenic fungus *Fusarium fujikuroi*, *Angew. Chem., Int. Ed.*, 2016, **55**, 8748.

25 S. W. Crossley, F. Barabe and R. A. Shenvi, Simple, chemoselective, catalytic olefin isomerization, *J. Am. Chem. Soc.*, 2014, **136**, 16788.

26 S.-B. Mou, W. Xiao, H.-Q. Wang, S.-J. Wang and Z. Xiang, Syntheses of epoxyguaiane sesquiterpenes (–)-englerin A, (–)-oxyphyllol (+)-orientalol E, and (+)-orientalol F: a synthetic biology approach, *Org. Lett.*, 2020, **22**, 1976.

27 S.-B. Mou, W. Xiao, H.-Q. Wang, K.-Y. Chen and Z. Xiang, Syntheses of the carotene-type terpenoids (+)-schisanwilsonene A and (+)-tormesol via a two-stage approach, *Org. Lett.*, 2021, **23**, 400.

28 P. Rabe, J. Rinkel, T. A. Klapchinski, L. Barra and J. S. Dickschat, A method for investigating the stereochemical course of terpene cyclisations, *Org. Biomol. Chem.*, 2016, **14**, 158.

29 B. H. Long, J. M. Carboni, A. J. Wasserman, L. A. Cornell, A. M. Casazza, P. R. Jensen, T. Lindel, W. Fenical and C. R. Fairchild, Eleutherobin, a novel cytotoxic agent that induces tubulin polymerization, is similar to paclitaxel (Taxol), *Cancer Res.*, 1998, **58**, 1111.

30 K. C. Nicolaou, J. Pfefferkorn, J. Xu, N. Winssinger, T. Ohshima, S. Kim, S. Hosokawa, D. Vourloumis, F. van Delft and T. Li, Total synthesis and chemical biology of the sarcodictyins, *Chem. Pharm. Bull.*, 1999, **47**, 1199.

31 P. D. Scesa, Z. Lin and E. W. Schmidt, Ancient defensive terpene biosynthetic gene clusters in the soft corals, *Nat. Chem. Biol.*, 2022, **18**, 659.

32 B.-W. Chen, *et al.*, Klysimplexins I–T, eunicellin-based diterpenoids from the cultured soft coral *Klyxum simplex*, *Org. Biomol. Chem.*, 2011, **9**, 834.

33 P. D. Scesa and E. W. Schmidt, Biomimetic approach to diverse coral diterpenes from a biosynthetic scaffold, *Angew. Chem., Int. Ed.*, 2023, **62**, e202311406.

34 G. Siedenburg and D. Jendrossek, Squalene-hopene cyclases, *Appl. Environ. Microbiol.*, 2011, **77**, 3905.



35 S. C. Hammer, P.-O. Syréen, M. Seitz, B. M. Nestl and B. Hauer, Squalene hopene cyclases: highly promiscuous and evolvable catalysts for stereoselective C–C and C–X bond formation, *Curr. Opin. Chem. Biol.*, 2013, **17**, 293.

36 (a) S. C. Hammer, A. Marjanovic, J. M. Dominicus, B. M. Nestl and B. Hauer, Squalene hopene cyclases are protonases for stereoselective Brønsted acid catalysis, *Nat. Chem. Biol.*, 2015, **11**, 121; (b) A. Schneider, C. Curado, T. B. Lystbaek, S. Osuna and B. Hauer, Harnessing the structure and dynamics of the squalene-hopene cyclase for (–)-ambroxide production, *Angew. Chem., Int. Ed.*, 2023, **62**, e202301607; (c) M. Eichenberger, *et al.*, Asymmetric cation-olefin monocyclization by engineered squalene-hopene cyclases, *Angew. Chem., Int. Ed.*, 2021, **60**, 26080.

37 W. Xiao, S.-J. Wang, M.-Z. Yu, X.-J. Zhang and Z. Xiang, Chemoenzymatic synthesis of (+)-isoagatholactone, (+)-spongian-16-one, and 3-deoxychevalone A via biocatalytic polyene cyclization, *Org. Biomol. Chem.*, 2023, **21**, 5527.

38 K. Iwasaki, K. K. Wan, A. Oppedisano, S. W. M. Crossley and R. A. Shenvi, Simple, chemoselective hydrogenation with thermodynamic stereocontrol, *J. Am. Chem. Soc.*, 2014, **136**, 1300.

39 W. Du, Z. Cheng, X. Pan, C. Liu, M. Yue, T. Li, Z. Xiao, L.-L. Li, X. Zeng, X. Lin, F. Li and L.-B. Dong, Microbe engineering to provide drimane-type building blocks for chiral pool synthesis of meroterpenoids, *Angew. Chem., Int. Ed.*, 2025, **64**, e202419463.

40 F.-R. Li, X. Lin, Q. Yang, N.-H. Tan and L.-B. Dong, Efficient production of clerodane and *ent*-kaurane diterpenes through truncated artificial pathways in *Escherichia coli*, *Beilstein J. Org. Chem.*, 2022, **18**, 881.

41 X. Wang, J. H. Pereira, S. Tsutakawa, X. Fang, P. D. Adams, A. Mukhopadhyay and T. S. Lee, Efficient production of oxidized terpenoids via engineering fusion proteins of terpene synthase and cytochrome P450, *Metab. Eng.*, 2021, **64**, 41.

42 T.-H. Chen, C.-T. Chen, C.-F. Lee, R.-J. Huang, K.-L. Chen, Y.-C. Lu, S.-Y. Liang, M.-T. Pham, Y. K. Rao, S.-H. Wu, R.-J. Chein and H.-C. Lin, The biosynthetic gene cluster of mushroom-derived antrocin encodes two dual-functional haloacid dehalogenase-like terpene cyclases, *Angew. Chem., Int. Ed.*, 2023, **62**, e202215566.

43 (a) D. J. Weix, Methods and mechanisms for cross-electrophile coupling of  $Csp^2$  halides with alkyl electrophiles, *Acc. Chem. Res.*, 2015, **48**, 1767; (b) D. A. Everson and D. J. Weix, Cross-electrophile coupling: principles of reactivity and selectivity, *J. Org. Chem.*, 2014, **79**, 4793.

44 (a) Y. Wei, E. L. Ang and H. Zhao, Recent developments in the application of P450 based biocatalysts, *Curr. Opin. Chem. Biol.*, 2018, **43**, 1; (b) R. Fasan, Tuning P450 enzymes as oxidation catalysts, *ACS Catal.*, 2012, **2**, 647.

45 (a) R. P. Hausinger, Fe(II)/a-ketoglutarate-dependent hydroxylases and related enzymes, *Crit. Rev. Biochem. Mol. Biol.*, 2004, **39**, 21–68; (b) C. R. Zwick, III and H. Renata, Harnessing the biocatalytic potential of iron- and a-ketoglutarate-dependent dioxygenases in natural product total synthesis, *Nat. Prod. Rep.*, 2020, **37**, 1065.

46 (a) C. J. C. Whitehouse, S. G. Bell and L.-L. Wong, P450BM3 (CYP102A1): connecting the dots, *Chem. Soc. Rev.*, 2011, **41**, 1218; (b) G.-R. Roiban and M. T. Reetz, Expanding the toolbox of organic chemists: directed evolution of P450 monooxygenases as catalysts in regio- and stereoselective oxidative hydroxylation, *Chem. Commun.*, 2015, **51**, 2208.

47 Z. G. Brill, M. L. Condakes, C. P. Ting and T. J. Maimone, Navigating the chiral pool in the total synthesis of complex terpene natural products, *J. Am. Chem. Soc.*, 2017, **117**, 11753.

48 D. D. Dixon, J. W. Lockner, Q. Zhou and P. S. Baran, Scalable, divergent synthesis of meroterpenoids via “borono-sclareolide”, *J. Am. Chem. Soc.*, 2012, **134**, 8432.

49 (a) M. S. Chen and M. C. White, Combined effects on selectivity in Fe-catalyzed methylene oxidation, *Science*, 2010, **327**, 566; (b) R. K. Quinn, *et al.*, Site-selective aliphatic C–H chlorination using N-chloroamides enables a synthesis of chlorolissoclimide, *J. Am. Chem. Soc.*, 2016, **138**, 696; (c) Y. Kawamata, *et al.*, Scalable, electrochemical oxidation of unactivated C–H bonds, *J. Am. Chem. Soc.*, 2017, **139**, 7448; (d) N. D. Chiappini, J. B. C. Mack and J. Du Bois, Intermolecular C(sp<sup>3</sup>)–H amination of complex molecules, *Angew. Chem., Int. Ed.*, 2018, **57**, 4956.

50 K. Zhang, S. El Damaty and R. Fasan, P450 fingerprinting method for rapid discovery of terpene hydroxylating P450 catalysts with diversified regioselectivity, *J. Am. Chem. Soc.*, 2011, **133**, 3242.

51 J. Li, F. Li, E. King-Smith and H. Renata, Merging Chemoenzymatic and Radical-Based Retrosynthetic Logic for Rapid and Modular Synthesis of Oxidized Meroterpenoids, *Nat. Chem.*, 2020, **12**, 173.

52 J. C. Lo, *et al.*, Fe-catalyzed C–C bond construction from olefins via radicals, *J. Am. Chem. Soc.*, 2017, **139**, 2484.

53 D. A. Everson, R. Shrestha and D. J. Weix, Nickel-catalyzed reductive cross-coupling of aryl halides with alkyl halides, *J. Am. Chem. Soc.*, 2010, **132**, 920.

54 H. Yokoe, *et al.*, Enantiocontrolled total syntheses of breviones A, B, and C, *J. Am. Chem. Soc.*, 2011, **133**, 8854.

55 J. Li, F. Chen and H. Renata, Concise Chemoenzymatic Synthesis of Gedunin, *J. Am. Chem. Soc.*, 2022, **144**, 19238.

56 J. Feng, V. J. Garza and M. J. Krische, Redox-triggered C–C coupling of alcohols and vinyl epoxides: diastereo- and enantioselective formation of all-carbon quaternary centers via tert-(hydroxy)-prenylation, *J. Am. Chem. Soc.*, 2014, **136**, 8911.

57 C. Petrier, C. Dupuy and J. L. Luche, Conjugate additions to a,b-unsaturated carbonyl compounds in aqueous media, *Tetrahedron Lett.*, 1986, **27**, 3149.

58 Y. You, X.-J. Zhang, W. Xiao, T. Kunthic, Z. Xiang and C. Xu, Unified enantiospecific synthesis of drimane meroterpenoids enabled by enzyme catalysis and transition metal catalysis, *Chem. Sci.*, 2024, **15**, 19307.

59 (a) M. G. L. Henquet, *et al.*, Identification of a drimenol synthase and drimenol oxidase from *Persicaria hydropiper*, involved in the biosynthesis of insect deterrent drimanes, *Plant J.*, 2017, **90**, 1052; (b) M. Kwon, S. A. Cochrane,



J. C. Vederas and D.-K. Ro, Molecular cloning and characterization of drimenol synthase from valerian plant (*Valeriana officinalis*), *FEBS Lett.*, 2014, **588**, 4597; (c) N. N. Q. Vo, Y. Nomura, K. Kinugasa, H. Takagi and S. Takahashi, Identification and characterization of bifunctional drimenol synthases of marine bacterial origin, *ACS Chem. Biol.*, 2022, **17**, 1226; (d) Y. Huang, S. Hoefgen and V. Valiante, Biosynthesis of fungal drimane-type sesquiterpene esters, *Angew. Chem., Int. Ed.*, 2021, **60**, 23763.

60 D. J. Charboneau, E. L. Barth, N. Hazari, M. R. Uehling and S. L. Zultanski, A widely applicable dual catalytic system for cross-electrophile coupling enabled by mechanistic studies, *ACS Catal.*, 2020, **10**, 12642.

61 Z. Li, H. S. Park, J. X. Qiao, K.-S. Yeung and J.-Q. Yu, Ligand-enabled C–H hydroxylation with aqueous H<sub>2</sub>O<sub>2</sub> at room temperature, *J. Am. Chem. Soc.*, 2022, **144**, 18109.

62 A. H. De Boer and I. J. de Vries-van Leeuwen, Fusicocanes: Diterpenes with surprising biological functions, *Trends Plant Sci.*, 2012, **17**, 360.

63 (a) J. Ohkanda, Fusicoccin: A chemical modulator for 14-3-3 proteins, *Chem. Lett.*, 2021, **50**, 57; (b) A. Sengupta, J. Liriano, E. A. Bienkiewicz, B. G. Miller and J. H. Frederich, Probing the 14-3-3 isoform-specificity profile of protein–protein interactions stabilized by fusicoccin A, *ACS Omega*, 2020, **5**, 25029; (c) M. Molzan, S. Kasper, L. Rögl, M. Skwarczynska, T. Sassa, T. Inoue, F. Breitenbuecher, J. Ohkanda, N. Kato, M. Schuler and C. Ottmann, Stabilization of physical RAF/14-3-3 interaction by cotylenin A as treatment strategy for RAS mutant cancers, *ACS Chem. Biol.*, 2013, **8**, 1869.

64 Y. Jiang and H. Renata, Modular Chemoenzymatic Synthesis of Ten Fusicocane Diterpenoids, *Nat. Chem.*, 2024, **16**, 1531.

65 Y. Ono, A. Minami, M. Noike, Y. Higuchi, T. Toyomasu, T. Sassa, N. Kato and T. Dairi, Dioxygenases, key enzymes to determine the aglycon structures of fusicoccin and brassicene, diterpene compounds produced by fungi, *J. Am. Chem. Soc.*, 2011, **133**, 2548.

66 N. Kato, H. Okamoto and T. Takeshita, Total synthesis of optically active cotylenol, a fungal metabolite having a leaf growth activity. Intramolecular ene reaction for an eight-membered ring formation, *Tetrahedron*, 1996, **52**, 3921.

67 R. Zalot, N. Oberg and J. A. Gerlt, The EFI web resource for genomic enzymology tools: Leveraging protein, genome, and metagenome databases to discover novel enzymes and metabolic pathways, *Biochemistry*, 2019, **58**, 4169.

68 M. Uwamori, R. Osada, R. Sugiyama, K. Nagatani and M. Nakada, Enantioselective total synthesis of cotylenin A, *J. Am. Chem. Soc.*, 2020, **142**, 5556.

69 J.-Q. Yu and E. J. Corey, Diverse pathways for the palladium(II)-mediated oxidation of olefins by tert-butylhydroperoxide, *Org. Lett.*, 2002, **4**, 2727.

70 Y. Tang, *et al.*, Structural revisions of a class of natural products: scaffolds of aglycon analogues of fusicoccins and cotylenins isolated from fungi, *Angew. Chem., Int. Ed.*, 2016, **55**, 4069.

71 S. Isayama and T. Mukaiyama, A new method for preparation of alcohols from olefins with molecular oxygen and phenylsilane by the use of bis(acetylacetonato)cobalt(II), *Chem. Lett.*, 1989, 1071.

72 B. Botta, G. D. Monache, D. Misiti, A. Vitali and G. Zappia, Aryltetralin lignans: chemistry, pharmacology and biotransformations, *Curr. Med. Chem.*, 2001, **8**, 1363.

73 J. Li, X. Zhang and H. Renata, Asymmetric chemoenzymatic synthesis of (–)-podophyllotoxin and related aryltetralin lignans, *Angew. Chem., Int. Ed.*, 2019, **58**, 11657.

74 W. Lau and E. S. Sattely, Six enzymes from mayapple that complete the biosynthetic pathway to the etoposide aglycone, *Science*, 2015, **349**, 1224.

75 M. P. DeMartino, K. Chen and P. S. Baran, Intermolecular enolate heterocoupling: scope, mechanism and application, *J. Am. Chem. Soc.*, 2008, **130**, 11546.

76 M. Lazzarotto, L. Hammerer, M. Heetmann, A. Borg, L. Schmermund, L. Steiner, P. Hartmann, F. Belaj, W. Kroutil, K. Gruber and M. Fuchs, Chemoenzymatic total synthesis of deoxy-, epi- and podophyllotoxin and a biocatalytic kinetic resolution of dibenzylbutyrolactones, *Angew. Chem., Int. Ed.*, 2019, **58**, 8226.

77 K. H. Gibson, Prostaglandins, thromboxanes, PGX: biosynthetic products from arachidonic acid, *Chem. Soc. Rev.*, 1977, **6**, 489.

78 C. Tanase, L. Pintilie and R. E. Tanase, Lactones in the synthesis of prostaglandins and prostaglandin analogs, *Int. J. Mol. Sci.*, 2021, **22**, 1572.

79 Y. Yin, J. Wang and J. Li, A concise and scalable chemoenzymatic synthesis of prostaglandins, *Nat. Commun.*, 2024, **15**, 2523.

80 F. Theil, H. Schick, G. Winter and G. Reck, Lipase-catalyzed trans-esterification of meso-cyclopentane diols, *Tetrahedron*, 1991, **47**, 7569.

81 C. V. F. Baldwin, R. Wohlgemuth and J. M. Woodley, The first 200-L scale asymmetric Baeyer–Villiger oxidation using a whole-cell biocatalyst, *Org. Process Res. Dev.*, 2008, **12**, 660.

82 E. Vitaku, D. T. Smith and J. T. Njardarson, Analysis of the structural diversity, substitution patterns, and frequency of nitrogen heterocycles among U.S. FDA approved pharmaceuticals, *J. Med. Chem.*, 2014, **57**, 10257.

83 (a) M. A. Larsen, E. T. Hennessy, M. C. Deem, Y. Lam, J. Sauri and A. C. Sather, A modular and diastereoselective 5 + 1 cyclization approach to N-(hetero)aryl piperidines, *J. Am. Chem. Soc.*, 2020, **142**, 726; (b) T. Sandmeier, S. Krautwald and E. M. Carreira, Stereoselective synthesis of piperidines by iridium-catalyzed cyclocondensation, *Angew. Chem., Int. Ed.*, 2017, **56**, 11515; (c) P. M. Weintraub, J. S. Sabol, J. M. Kane and D. R. Borchering, Recent advances in the synthesis of piperidones and piperidines, *Tetrahedron*, 2003, **59**, 2953; (d) X. Ma, I. R. Hazelden, T. Langer, R. H. Munday and J. F. Bower, Enantioselective aza-Heck cyclizations of N-(tosyloxy)carbamates: synthesis of pyrrolidines and piperidines, *J. Am. Chem. Soc.*, 2019, **141**, 3356; (e) G. Bertuzzi, L. Berbardi and M. Fochi, Nucleophilic dearomatization of activated pyridines, *Catalysts*, 2018, **8**, 632; (f) J. A. Bull,



J. J. Mousseau, G. Pelletier and A. B. Charette, Synthesis of pyridine and dihydropyridine derivatives by regio- and stereo-selective addition to N-activated pyridines, *Chem. Rev.*, 2012, **112**, 2642.

84 J. He, K. Yokoi, B. Wixted, B. Zhang, Y. Kawamata, H. Renata and P. S. Baran, Biocatalytic C–H oxidation meets radical cross-coupling: simplifying complex piperidine synthesis, *Science*, 2024, **386**, 1421.

85 J. Mattay and W. Hüttel, Pipelicolic acid hydroxylases: a monophyletic clade among *cis*-selective bacterial proline hydroxylates that discriminates L-proline, *ChemBioChem*, 2017, **18**, 1523.

86 M. Hibi, R. Mori, R. Miyake, H. Kawabata, S. Kozono, S. Takahashi and J. Ogawa, Novel enzyme family found in filamentous fungi catalyzing trans-4-hydroxylation of L-pipelicolic acid, *Appl. Environ. Microbiol.*, 2016, **82**, 2070.

87 (a) S. Shinoda, A. Itakura, H. Sasano, R. Miyake, H. Kawabata and Y. Asano, Rational design of the soluble variant of L-pipelicolic acid hydroxylase using the a-helix rule and the hydrophobicity contradiction rule, *ACS Omega*, 2022, **7**, 29508; (b) J. Nazor, R. Osborne, J. Liang, J. Vroom, X. Zhang, D. Entwistle, R. Voladri, R. D. Garcia, J. C. Moore, S. Grosser, B. Kosjek and M. Truppo, *Biocatalysts and methods for hydroxylation of chemical compounds*, US Pat., 10184117B2, 2019.

88 N. Widderich, A. Höppner, M. Pittelkow, J. Heider, S. H. J. Smits and E. Bremer, Biochemical properties of ectoine hydroxylases from extremophiles and their wider taxonomic distribution among microorganisms, *PLoS One*, 2014, **9**, e93809.

89 (a) S. J. Harwood, M. D. Palkowitz, C. N. Gannett, P. Perez, Z. Yao, L. Sun, H. D. Abruna, S. L. Anderson and P. S. Baran, Modular terpene synthesis enabled by mild electrochemical couplings, *Science*, 2022, **375**, 745; (b) M. D. Palkowitz, *et al.*, Overcoming limitations in decarboxylative arylation, *J. Am. Chem. Soc.*, 2022, **144**, 17709.

90 K. D. Cusick and G. S. Sayler, An overview of the marine neurotoxin, saxitoxin: genetics, molecular targets, methods of detection and ecological functions, *Mar. Drugs*, 2013, **11**, 991.

91 Y. Guo, Y. Li, S. Chen, O. Poll, Y. Wu, C. Prier, K.-J. Xiao and P. S. Baran, *Scalable, convergent total synthesis of (+)-saxitoxin and related natural products*, *ChemRxiv*, 2025, DOI: [10.26434/chemrxiv-2025-qj8f5](https://doi.org/10.26434/chemrxiv-2025-qj8f5).

92 (a) S. Ni, *et al.*, A general amino acid synthesis enabled by innate radical cross-coupling, *Angew. Chem., Int. Ed.*, 2018, **57**, 14560; (b) S. Ni, *et al.*, A radical approach to anionic chemistry: synthesis of ketones, alcohols and amines, *J. Am. Chem. Soc.*, 2019, **141**, 6726.

93 (a) B. E. Murray, L. I. Penabad and R. T. Kennedy, Advances in coupling droplet microfluidics to mass spectrometry, *Curr. Opin. Biotechnol.*, 2023, **82**, 102962; (b) A. Jain, S. Stavrakis and A. DeMello, Droplet-based microfluidics and enzyme evolution, *Curr. Opin. Biotechnol.*, 2024, **87**, 103097.

94 A. Paton, D. Boiko, J. Perkins, N. Cemalovic, T. Reschützegger, G. Gomes and A. Narayan, *Generation of connections between protein sequence space and chemical space to enable a predictive model for biocatalysis*, *ChemRxiv*, 2025, DOI: [10.26434/chemrxiv-2024-w4dtr](https://doi.org/10.26434/chemrxiv-2024-w4dtr).

95 (a) M. A. Emmanuel, *et al.*, Photobiocatalytic strategies for organic synthesis, *Chem. Rev.*, 2023, **9**, 5459; (b) F. Liu, X. Peng, J. Yu and X. Huang, Recent advances in repurposing natural enzymes for new-to-nature asymmetric photobiotransformations, *Org. Chem. Front.*, 2025, DOI: [10.1039/D5Q00470E](https://doi.org/10.1039/D5Q00470E).

96 N. J. Turner and E. O'Reilly, Biocatalytic retrosynthesis, *Nat. Chem. Biol.*, 2013, **9**, 285.

